An Overview of Glycerol Electrooxidation Mechanisms on Pt, Pd and Au

Tianyu Li,*[a] David A. Harrington[a]
[a] Department of Chemistry, University of Victoria, Victoria, BC, Canada V8W 3V6
Email: tianyuli@uvic.ca, dharr@uvic.ca

January 10, 2021

Abstract

In the most recent decade, glycerol electrooxidation (GEOR) has attracted extensive research interest for valorization of glycerol, *i.e.*, the conversion of glycerol to value-added products. These reactions at platinum, palladium, and gold electrodes have a lot of uncertainty in their reaction mechanisms, which has generated some controversies. This review gathers many reported experimental results, observations and proposed reaction mechanisms in order to draw a full picture of GEOR. A particular focus is the clarification of two propositions: Pd is inferior to Pt in cleaving the C-C bonds of glycerol during the electrooxidation and the massive production of CO_2 at high overpotentials is due to the oxidation of the already-oxidized carboxylate products. It is concluded that the inferior C-C bond cleavability with Pd electrodes, as compared with Pt electrodes, is due to the inefficiency of deprotonation, and the massive generation of CO_2 as well as other C1/C2 side products is partially caused by the consumption of OH^- at the anodes, as a lower pH reduces the amount of carboxylates and favors the C-C bond scission. A reaction mechanism is proposed in this review, in which the generation of side products are directly from glycerol ("competition" between each side product) rather than from the further oxidation of C2/C3 products. Additionally, GEOR results and associated interpretations for Ni electrodes are presented, as well as a brief review on the performances of multi-metallic electrocatalysts (most of which are nanocatalysts) as an introduction to these future research hotpots.

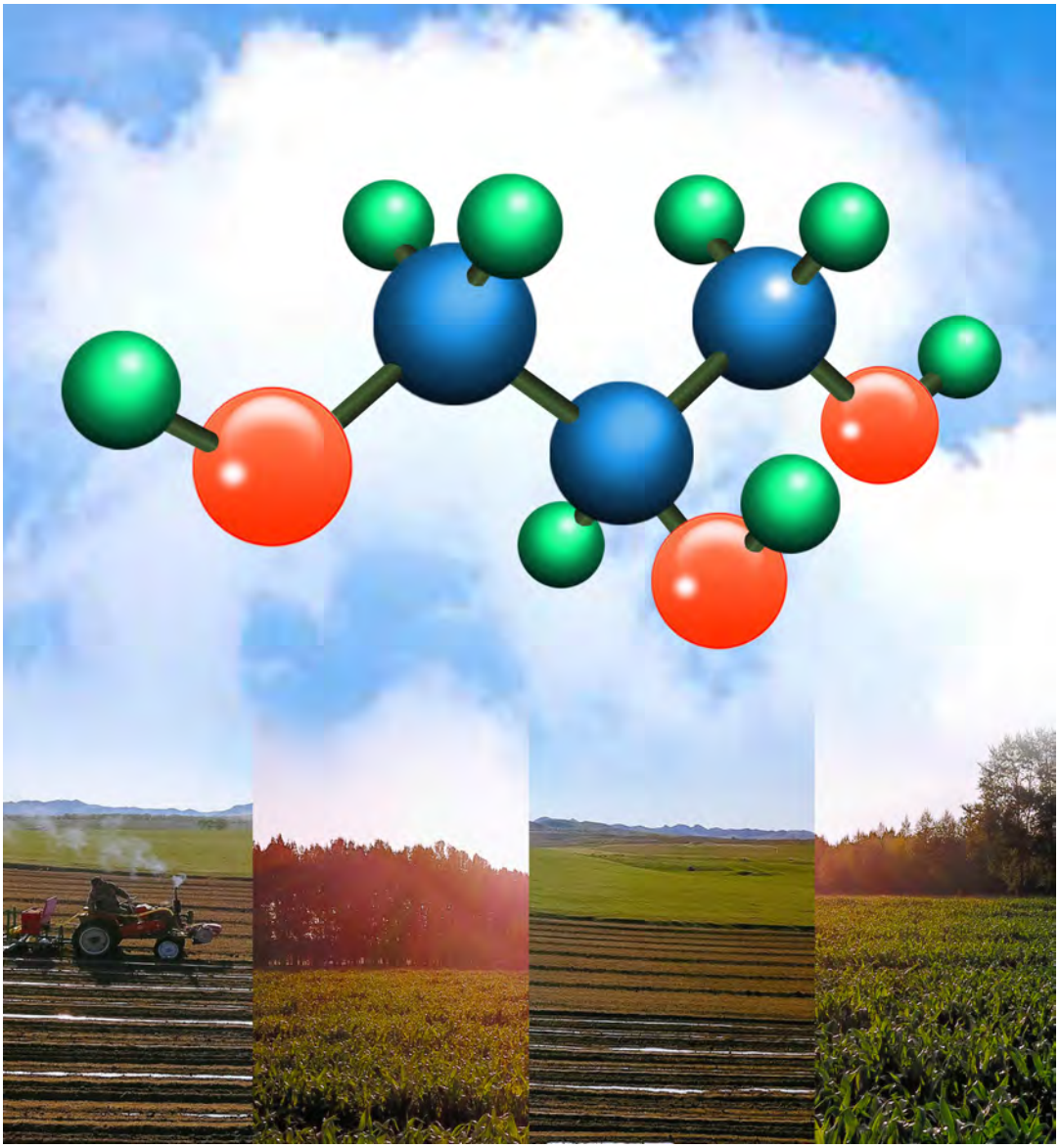

Author Biographies

Tianyu Li received his Bachelor of Science (B.Sc.) degree in Materials Science at Nanjing University. He recently completed his Ph.D. degree in Chemistry at the University of Victoria, specializing in the microfluidic devices for online detection of alcohol electrooxidation with Raman spectroscopy. He is currently a postdoctoral researcher at the University of Toronto.

David Harrington received his Ph.D. in Chemistry from the University of Auckland in 1982. After postdoctoral positions in the United States and Canada, he took up his present position at the University of Victoria, BC, Canada in 1987, where he is now a full professor. His research interests are in electrochemistry, microfluidics, and surface science as they apply to electrocatalysis, particularly oxidation of small organic molecules. He specializes in mechanistic electrochemical impedance spectroscopy, including its theory, applications, and development of dynamic impedance methods.

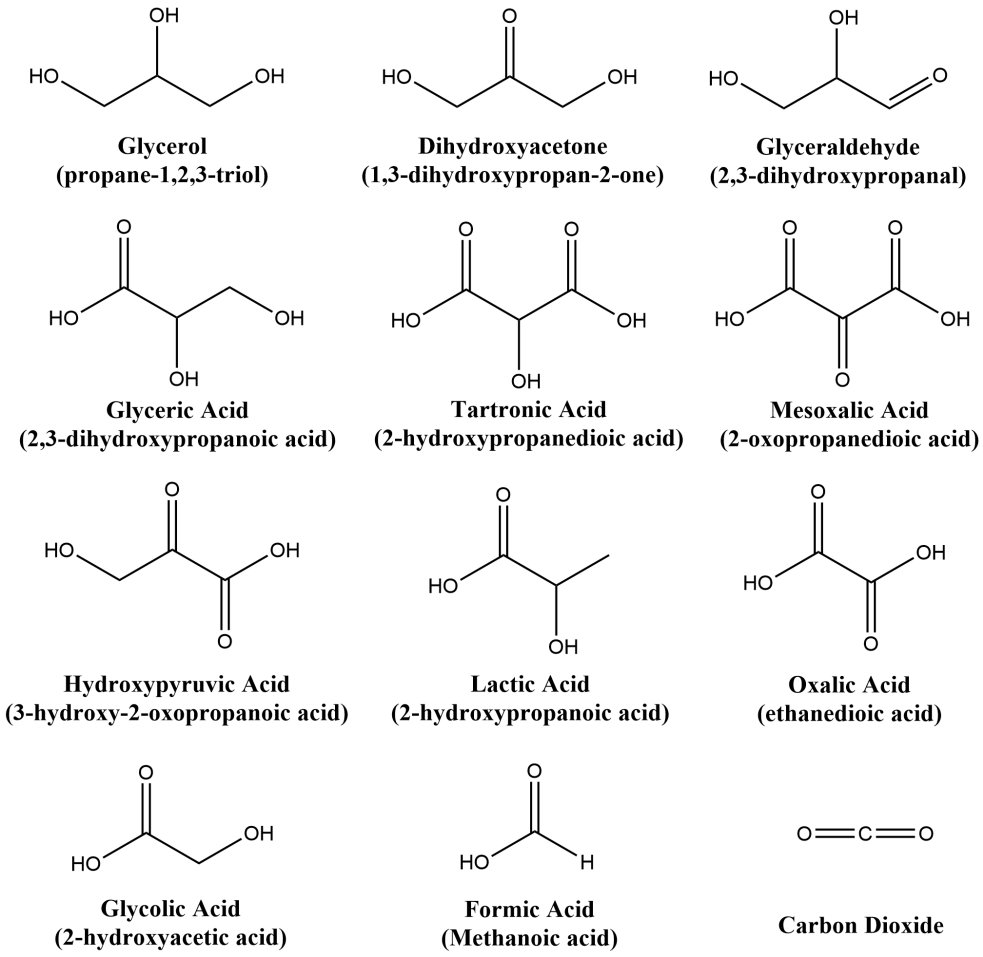

Figure 1: Molecular structures of glycerol and its oxidation products.

1 Introduction

Glycerol is produced on a large scale as a byproduct of biodiesel production, in the transterification of triglycerides with alcohols.[1] This makes it a cheap and useful starting point for conversion into value-added products ("valorization") such as dihydroxyacetone, glyceraldehyde, glyceric acid, glycolic acid, lactic acid, hydroxypyruvic acid, and *etc* (see Figure 1).[2] Previously, glycerol oxidation for valorization and energy generation has been implemented with many non-electrochemical methods. However, most of these have disadvantages such as requiring high temperature, high pressure, an external oxygen supply, or even use of heavy metals.[3] Compared with those harsh reaction conditions that are hard to maintain or toxicity that poses a threat to human health, electrooxidation of glycerol (GEOR) occurs under mild conditions and avoids those requirements.

There has been a rapid increase in the number of GEOR studies since 2010 (Figure 2a). Among the Scientific-Citation-Indexed studies on GEOR, most of which were done with highly catalytically active noble metals (*e.g.* platinum, palladium, and gold) for high efficiencies. However, as a non-noble metal abundant on earth, nickel has been receiving more and more attention (see Figure 2b).

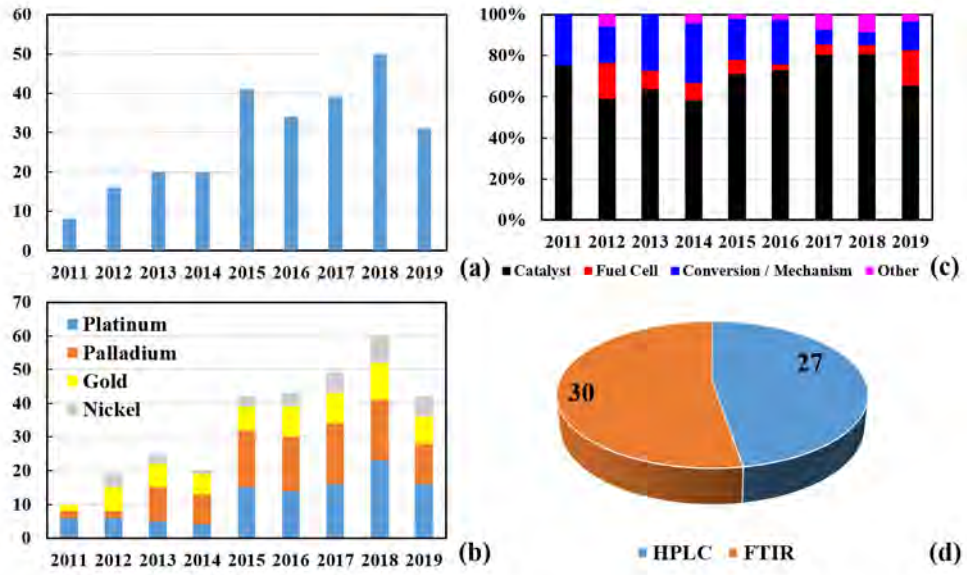

Figure 2: Statistical data of Scientific-Citation-Indexed (SCI) publications about glycerol electrooxidation since 2011. (a) Numbers of Scientific-Citation-Indexed (SCI) publications from 2011 to Jul 2019 found on Web of Science using the keyword "glycerol electrooxidation". (b) Numbers of GEOR studies conducted with Pt-based, Pd-based, Au-based, and Ni-based electrocatalysts from 2011 to Jul 2019. (c) Portions of GEOR studies focusing on catalysts, fuel cells, conversion / mechanism and *etc*, from 2011 to Jul 2019. (d) Portions of mechanism or conversion studies using HPLC or FTIR.

Nickel used to be utilized synergistically with noble metals,[4–6] but, its high activity of electrocatalyzing GEOR alone has made it a promising substitute for noble metals.[7–9] With metallic electrocatalysts offering high efficiency in GEOR, studies conducted by researchers worldwide have covered all aspects related to GEOR, including novel nanocatalysts enhancing the efficiency and selectivity of GEOR towards certain products,[10–12] product distribution analysis for the determination of the reaction mechanisms and kinetics,[13,14] and fuel cell fabrications (theoretically generating 1.01 V),[15–17] as shown in Figure 2c. Among them, the selectivity of glycerol oxidation products (usually reported with HPLC or FTIR data as illustrated in Figure 2d) is of great interest as it directly influences the potential for commericial production of value-added products.

To obtain a high selectivity towards certain value-added products, reaction mechanism studies should be a prerequisite, but they are considerably outnumbered by papers describing empirical discoveries of novel electrocatalysts.[1,18] Moreover, the previously reported GEOR mechanisms with Pt, Pd, and Au are plagued by the fact that many hypotheses, observations and results are contradictory to each other. The innovations in new catalysts has somewhat worsened this issue as their preparation processes are under disparate conditions, and reporting of elemental compositions, morphologies and crystal planes have not been standardized.[18]

An overview of these hypotheses and controversies is therefore timely, and should be used to direct the future works. It is an area that has not yet been emphasized in previously published reviews.[19–21] The reaction mechanism of GEOR was partially reviewed by Gomes et al.[22] together

with other C3 alcohols. Different chemisorption assumptions are covered, including the adsorption via both terminal carbon atoms, or through one terminal carbon atom and the secondary carbon atom. In recently published reviews, Coutanceau et al.[23] categorized GEOR processes into two categories, that is, acidic and alkaline electrolytes, together with the performances of different metal catalysts. Baranova et al. presented a very broad survery of literatures reporting the product distribution of glycerol oxidation at various catalysts.[24] Du et al.[3] reviewed Pt-based, Pd-based and Au-based catalysts and proposed that higher pH and overpotentials tend to generate more highly oxidized products. Those reviews have nicely summarized the reported product distributions, but a comprehensive understanding of the mechanism remains elusive. A recent article in *Encyclopedia of Interfacial Chemistry* by Angelucci et al. provides a good overview and summarizes most of the reported observations and accepted mechanisms in GEOR studies on Au, Pt, Pd and Ag.[25] Also, a noteworthy overview was given by Martins et al.[18] as a chapter of the book *Increased Biodiesel Efficiency*. The overview ranges from reaction mechanisms to the types of electrocatalysts, and to the performances of glycerol-based fuel cells. Instead of giving detailed experimental conditions and comparing product distributions, only a few widely recognized observations and explanations are mentioned (*e.g.* enhanced selectivity towards DHA by adding Bi atoms to (111) planes). They concluded that the reaction mechanisms of GEOR are still far from fully understood .

Herein, an overview of GEOR conducted with Pt, Pd and Au catalysts is presented as an attempt to elucidate GEOR more comprehensively by presenting a comprehensive mechanistic scheme based on previously reported GEOR results by researchers worldwide. The content of this review includes: (1) summaries of the observations, hypotheses and controversies of GEOR brought by researchers in the most recent decade, (2) elucidations and clarifications of two propositions that prevail in the field of GEOR at Pt and Pd electrodes, (3) a proposed reaction mechanism arguing that the generation of C1/C2 products are directly from glycerol rather than from the electrooxidation of C2/C3 side products, and therefore the generation of a C1/C2 product is competing with other products generated through parallel pathways. For completeness, mechanisms for Ni-based GEOR and properties of nanocatalysts are also discussed.

2 Summary of Observed Glycerol Oxidation Results and Reported Reaction Mechanisms

Benefitting from the high reactivity induced by the adjacent hydroxyl groups,[26–28] glycerol enjoys the potential of being oxidized into multiple intermediates/products, most of which are favored in industry because of the added commercial value. Pt, Pd and Au are noble metallic catalysts commonly used for electrocatalytically oxidizing glycerol.[29,30] Based on hundreds of experimental observations, reaction mechanisms have been proposed by researchers worldwide to elucidate the oxidation processes. However, as concluded by Angelucci et al.,[25] there is still much unknown nature of the surface-adsorbed species, which is the main challenge in deeply understanding the reaction mechanism of GEOR on noble metals. In this section, controversies and hypotheses are reviewed to give a comprehensive elucidation of GEOR mechanisms presented so far.

2.1 Platinum

In general, the electrocatalytic oxidation of alcohol can be divided into four steps: dissociative adsorption, bond breaking / electron transfer, reaction between oxygenated species and functional groups of adsorbed species on the surface, and intermediate/final product desorption.[22] Different adsorption pathways may lead to different adsorbates (*e.g.* alkoxide, acyl, aldehydes, etc.[31]), and presumably different products. Among all noble metallic catalysts, Pt is considered as the

most active one due to its low d-band center (-2.25 eV)[32] which favors deprotonation. According to researchers, the reaction pathways of GEOR with Pt can be categorized into two groups: O-adsorption (happening at higher overpotentials through the coordination of a lone pair of oxygen electrons in the hydroxyl group) and C-adsorption (major pathway at lower overpotentials) whose adsorbates are reportedly more stable than O-adsorbates in acidic medium.[33]

O-adsorption (Figure 3a) involves the deprotonation of the primary or the secondary hydroxyl group to produce alkoxide. Kwon et al.[34] reported that strong alkali can promote this deprotonation step, since glycerol behaves as a weak acid in a strong alkaline solution whose pH is close to the pKa of glycerol (14.15). Once chemisorbed, a second deprotonation from the carbon atom occurs, which oxidizes glycerol into glyceraldehyde or DHA.[19] As in alkaline conditions OH^- exists in the electrolyte, Pt-OH(ads) (reportedly produced at 0.5 V – 0.6 V vs RHE[20]) can subsequently oxidize the chemisorbed glyceraldehyde into glyceric acid or glycerate. It is also known that in strong base, the Cannizzaro reaction can convert aldehyde to carboxylic acid (or to carboxylate in alkali) and alcohol[35]. Similaly, glyceraldehyde and DHA can be chemically converted to lactic acid through 2-hydroxypropenal or pyruvaldehyde (produced from based-catalyzed dehydrated glyceraldehyde or DHA).[36–38] (As emphasized by Koper's group, the chemical conversion of soluble intermediates can sometimes lead to misinterpretion of results by researchers.[35]) However, no scission of the C-C bond occurs in either sub-pathway.

In the case of C-adsorption (Figure 3b), Koper et al.[33] and Sieben et al.[39] showed that in acidic conditions Pt(100) only chemisorbs a terminal carbon atom of glycerol and oxidizes it into glyceraldehyde with partial deprotonation, whereas Pt(111) chemisorbs both types of carbon atoms either individually or through two Pt-C bonds producing an enediol-like intermediate for the oxidation to DHA[40] and glyceraldehyde. Besides, as found by Koper et al. and Greeley et al., another intermediate that is adsorbed onto Pt(111) by two terminal carbon atoms can be a poisoning species, as the following deprotonation is hard to proceed.[33,41,42] For those two intermediates to proceed to further deprotonation, two sub-pathways exist and take effect based on whether there is Pt-OH(ads). If not, since the C-C bond has been weakened by adsorption,[43] the breaking of the C-C bond can generate Pt-CO(ads) (surface-poisoning species) and Pt-R(ads) (C2 or C1 products), as shown in [Eq. (1)]. In fact, as reported by Greeley et al. in a DFT study[41], the transition state energies for breaking C-C bonds become much lower once the adsorbed glycerol has gone through several deprotonation steps, so that the scission of C-C bonds can occur at this stage and produce CO(ads) as a major product. Without extensive production of Pt-OH(ads) at higher overpotentials, Pt-CO(ads) ends up slowing down the oxidation.[12] In alkaline conditions, with the help of Pt-OH(ads), Pt-CO(ads) can react with Pt-OH(ads) to give CO_2 (Langmuir-Hinshelwood mechanism, [Eq. (2)]) or Pt-COOH(ads) (subsequently converted into carbonate, [Eqs. (3)-(5)]). It is widely hypothesized that the removal of CO is the rate-determining step of GEOR,[16] and therefore higher OH^- concentration leads to better catalytic activity because of the higher OH(ads) coverage and greater OH^- diffusion. Therefore, it is believed that the onset potential of OH adsorption has a negative correlation with pH, which also applies to Pd and Au.[15]

$$\mathrm{Pt-RCO(ads)} \rightarrow \mathrm{Pt-R(ads)} + \mathrm{Pt-CO(ads)} \tag{1}$$

$$\mathrm{Pt-CO(ads)} + \mathrm{Pt-OH(ads)} \rightarrow 2\mathrm{Pt} + \mathrm{CO_2}{+}\mathrm{H^+}{+}\mathrm{e^-} \tag{2}$$

$$\mathrm{Pt-CO(ads)} + \mathrm{Pt-OH(ads)} \rightarrow \mathrm{Pt} + \mathrm{Pt-COOH(ads)} \tag{3}$$

$$\mathrm{Pt-COOH(ads)} + \mathrm{Pt-OH(ads)} + 2\mathrm{OH^-} \rightarrow \mathrm{CO_3^{2-}}{+}2\mathrm{H_2O} \tag{4}$$

$$\mathrm{Pt-CO(ads)} + 2\mathrm{Pt-OH(ads)} + 2\mathrm{OH^-} \rightarrow \mathrm{CO_3^{2-}}{+}2\mathrm{H_2O} \tag{5}$$

In a hypothesis proposed by Roquet et al.,[44] C-adsorption may happen with both types of carbon atoms, implying the existence of multiple adsorbates. It is widely observed that glyceraldehyde

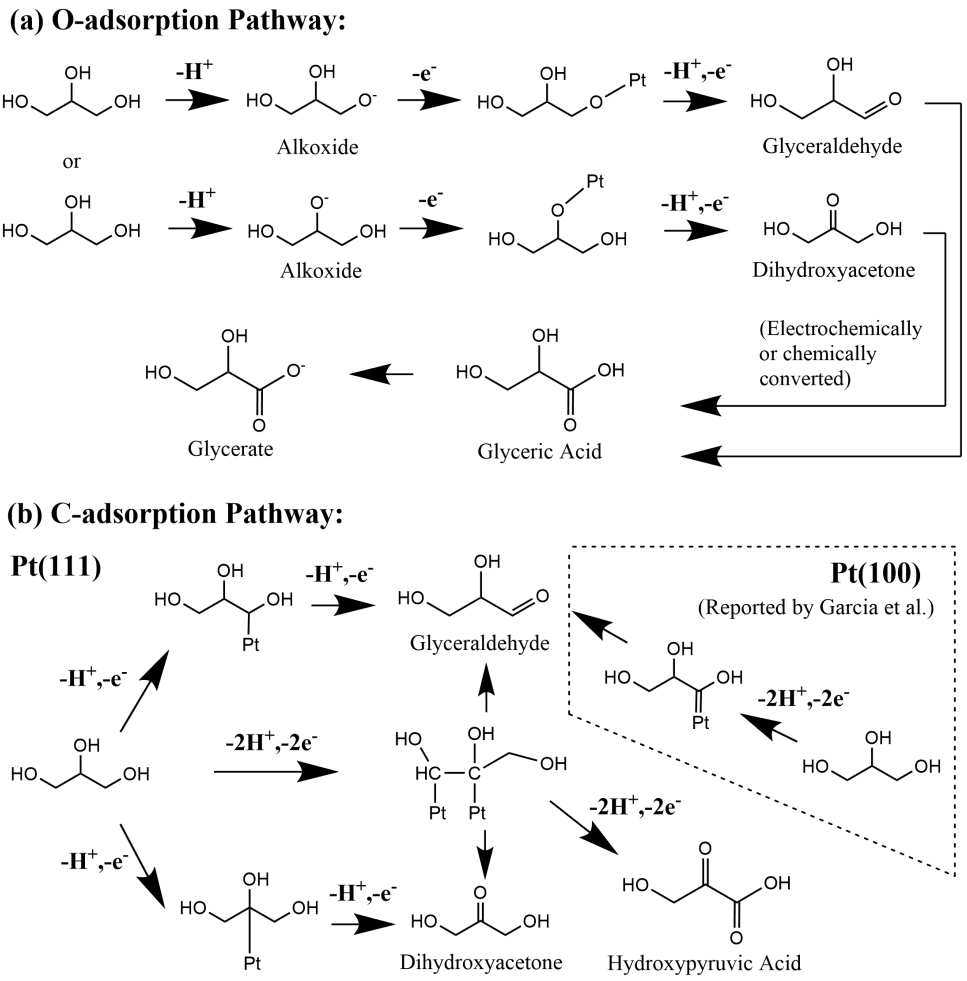

Figure 3: Pathways of glycerol electrooxidation at Pt electrodes. (a) O-adsorption, and (b) C-adsorption (adapted from Ref[33]).

and DHA are the two major intermediates, which indicates two major oxidation pathways, either through the primary alcohols or the secondary alcohol.[45] Dai et al[36] measured the product distribution of GEOR in alkali with Au-Pt nanoparticles using NMR spectra and HPLC. Their results show that the secondary alcohol oxidation occurs preferentially at lower overpotentials (0.45 V vs RHE) leading to DHA, whereas primary alcohol oxidation starts at higher overpotentials (0.9 V vs RHE), and generates mainly glyceric acid and tartronic acid. However, with both Pt and Pt-Cu electrodes, Ribeiro et al.[46] illustrated that glyceraldehyde was identified as the major oxidation product under acidic conditions, together with DHA and glyceric acid. These results derived by different research groups seem contradictory, but can be reconciled by assuming two co-existing effects. Firstly, a structural effect (two primary OH groups to one secondary OH group) makes the hydroxyl group on terminal carbon atoms more easily oxidized.[2,47] Secondly, secondary alcohol groups oxidize through simpler deprotonation steps.[48] Currently, an observation widely reported is the high selectivity towards DHA if metals like Bi, Ru and Sb are introduced to Pt(111) or polycrystalline Pt,[49–54] which indicates that the reaction pathway through primary alcohol oxidation is suppressed. A widely accepted mechanism interpreting this observation is that the adatoms disturb the three adjacent Pt sites which are needed for the oxidation of primary alcohols (see Section 5). However, Koper et al.[53] showed that Pb, In and Sn adatoms do not promote the GEOR selectivity towards DHA.

The ease of C-C bond cleavage is a controversial area that is still under debate and needs further investigation. The capability of an electrocatalyst to dissociate C-C bonds is usually estimated by calculating the ratio of C1/C2 products to C3 products.[2] The presence of CO(ads) can be taken as an indicator of bond cleavage.[55] Some observations suggest that this cleavage is favored at low overpotentials[16] and in acidic conditions,[36,56] which may be explained by the remarkable effect of oxygenated species on converting intermediates into carboxylates rather than breaking C-C bonds,[13] together with a possibly higher barrier for C-C cleavage in the presence of more OH(ads)/O(ads) at such overpotentials. Other researchers argue that large overpotentials overcome the energy barrier of C-C cleavage, as they observed massive production of CO_2 at potentials higher than 1.1 V vs RHE.[57,58]

Aside from pH and overpotential, other factors affecting the C-C bond dissociation have also been examined. A higher temperature can generally promote the oxidation of adsorbed species by enabling the energy barrier crossing, which is then followed by desorption of adsorbates. Ribeiro et al.[46] tested the effect of high temperature on C-C bond cleavage and concluded that high-temperature acts positively on this process as glycolic acid was found at the expense of glyceric acid. However, researchers have also reported a barely affected DHA selectivity over a range of temperatures up to 70°C using a Sb-modified Pt catalyst.[49]

Investigations of GEOR with Pt electrodes have involved both polycrystalline and monocrystalline (*e.g.* Pt(111), Pt(110), and Pt(100)) electrodes. Two CV peaks are shown during the anodic scan of GEOR at Pt(111) in acidic solution, which can be ascribed to the deprotonation of glycerol towards CO(ads) (0.56 V, broad and decreasing during continuous cycling) and the removal of CO(ads) with OH(ads) (0.78 V, sharp).[59] Spectroscopic (FTIR) studies show that bridge-bonded CO (CO_B) only exists on Pt(100) above 0.05 V vs RHE, and linearly bonded CO (CO_L) appears at higher overpotential, while Pt(111) and Pt(110) have only linearly absorbed CO.[33,58,60] Pt(111) was proven to be the most active plane for removal of CO and other intermediates.[16] Gomes et al.[61] reported that the dissociative adsorption and the breaking of C-C bonds are much easier on Pt(110) and Pt(100) than Pt(111), from which they argued that RCO(ads) is more stable on Pt(111). Angelucci et al.[62] also reported that acyl (Pt-RCO(ads)) groups are stable on Pt(111), and therefore O-adsorption is thought to be the major oxidation pathway through which the adsorbates generated are relatively more unstable.

On polycrystalline Pt, GEOR occurs by various reaction pathways, which occur at different

overpotentials.[63] Also, it is believed that the reaction processes on polycrystalline Pt are just the total of the reaction processes on the three different low index single-crystal faces. According to Fernandez et al.[63], the oxidation peak of GEOR below 0.8 V vs RHE is associated with defects in the (111) and (110) planes, whereas another peak at higher overpotentials (above 0.8 V vs RHE) is ascribed to the effect of Pt(100) defects.

At higher potential, Pt is oxidized to PtO, which is also regarded as an GEOR-active catalyst.[44] Dissociative adsorption of glycerol happens at the surface of PtO, with which both the primary carbon and secondary carbon are adsorbed onto two PtO sites. Nevertheless, only one proton is removed from each carbon adsorbed. The simultaneous reduction of PtO and oxidation of hydroxyl groups lead to Pt and a dissociated C-C bond, *i.e.* C1 or C2 products.

2.2 Palladium

Pd has a higher d-band center (-1.83 eV[32]) than Pt. Also, a difference between Pd and Pt is that on low index planes like (111) and (110), spectroscopic studies only show the existence of CO_B.[64,65] Pd only has linearly adsorbed CO at step and kink sites with low coordination numbers.[66,67]

One reaction mechanism proposed[68] is very much like the C-adsorption pathway in Pt-GEOR. However, Pd requires a more basic electrolyte as a promotor of this deprotonation process compared with Pt.[46] Nevertheless, excessive OH(ads) occupying the active sites may reduce the efficiency of GEOR.[69] Therefore, efficient GEOR on Pd depends on the presence of both Pd-OH(ads) and free Pd sites.[70] The reaction of Pd-RCO(ads) with Pd-OH(ads) is usually assumed to be the rate-determining step as on Pt ([Eqs. (6) and (7)])[71,72], but other researchers have hypothesized that the rate-determining step is the desorption of reaction intermediates (*e.g.* DHA at a low overpotential[73]).

$$\mathrm{Pd-(RCH_2OH)(ads)} + 3\mathrm{OH^-} \rightarrow \mathrm{Pd-RCO(ads)} + 3\mathrm{H_2O} + 3\mathrm{e^-} \tag{6}$$

$$\mathrm{Pd-RCO(ads)} + \mathrm{Pd-OH(ads)} \rightarrow \mathrm{Pd} + \mathrm{Pd-RCOOH(ads)} \tag{7}$$

Similar to Pt-GEOR, the production of CO_2 is usually seen at high overpotentials.[74] However, C-C bond dissociation is reportedly more difficult on Pd than Pt and Au,[15,75] which is supported by the observation that glyceric acid is more commonly produced on Pd than Pt.[46] In addition, oxygenated species are believed to facilitate C-C cleavage,[76,77] which is strongly contrasted by the negative role OH(ads) plays on C-C bond cleavage with Pt catalysts. Fortunately, the influence of the functional groups and the surface sites of Pd on C-C bond dissociation are much more deeply studied than on Pt catalysts. For example, Miller et al.[78] compared the C-C cleavability of ethanol and glycerol with Au@Pd nanoparticles (Pd shell covering Au core) and hypothesized that adjacent alcohol groups are needed for this bond cleavage. According to Coutanceau et al.[50], the cleavage of C-C bonds is subject to the adjacent sites on Pd terraces, as both the primary and secondary carbon atoms are supposed to be adsorbed on the crystal plane for this process. The preferential deposition of Bi on Pd(111) rather than Pd(100) remarkably reduces the availability of adjacent Pd atoms, therefore lowering the ability of C-C cleavage. With the change in the amount of deposited Bi, the surface rearrangement from Bi monomers to islands leads to fluctuation of Pd atom adjacency and consequently affects the C1/C2 selectivity.[14] Interestingly, GEOR occuring at Bi-modified Pt(111) electrode[79] has also been widely studied, which usually shows an increased DHA selectivity. However, the interpretation of this phenomenon given by Koper's group is that the adatoms of Bi promote the isomerization reaction of the enediol intermediate[33] towards DHA. In addition, Shishido et al.[80] tested the oxidation of glycerol on Bi-modified Pt (non-electrochemical) and found that the preferred conversion towards DHA is due to the chelation effect promoting the oxidation through secondary OH groups.

Additionally, a large number of studies have been directed to the catalytic activities of specific Pd crystal planes. For example, Pd(100), which is prominent in some nanostructured Pd catalysts,[52] is found to outperform Pd(111) in terms of the catalytic efficiency,[50,81,82] as it can adsorb glycerol more easily.[50,52] Furthermore, GEOR through the primary carbon on Pd(100) has been demonstrated in studies showing high selectivity towards glycerate[83] and tartronate.[84] In fact, comparative studies of the catalytic activity of different crystal planes of noble metals are highly valued in the illustration of reaction mechanisms, which include not only the comparison between undercoordinated planes like (111), (100) and (110), but also between low-index planes and high-index planes. For example, Pd(520), as a high-index plane with many kinks and steps which promote bond dissociation of glycerol, was found to have a higher catalytic activity compared to low-index planes.[11,85] However, the Fernández group tested the catalytic activity of Bi and Pb-modified Pt (both polycrystalline and low-index planes) and concluded that the undercoordinated planes are more electrocatalytically active in GEOR, once the poisoning effect is suppresed by the adatoms on such planes.[38] Their work is a reminder that any conclusions regarding the catalytic activity of certain crystal planes need to be made carefully, and the effect of adsorbates on the activity of electrodes needs to be considered.

2.3 Gold

The most important feature for GEOR occuring at Au electrodes is that GEOR only occurs with a noticeable current in alkaline media, and therefore most of the GEOR studies with Au electrodes are carried out in basic solutions. As shown by Koper et al.,[34] in strong alkaline condition the initial deprotonation of alcohol is catalyzed by base instead of metal (as mentioned above). Therefore the reactive species of GEOR in strong alkaline condition is glyceroate due to the deprotonation of H_α (scission of O-H). The electrooxidation continues with the deprotonation of H_β (C-H scission)[86]. According to Roy et al[87] and other researchers,[88] deprotonation of H_β is the rate-determining step of GEOR on Au, which differs completely from Pt and Pd.

Also, DFT studies showed that the adsorbed OH on Au surfaces lowers the activation barrier and thus facilitates the dissociation of C-H and O-H bonds[86]. In fact, researchers found that glycerol anchors to Au-OH(ads) for deprotonation and subsequent adsorption,[89–91] which leads to the production of glyceraldehyde at lower overpotentials in weak and strong alkaline conditions [Eq. (8-9)],[87] and therefore both OH(ads)-covered and free surface sites of Au must be present for the dissociative adsorption to proceed.[92] Fortunately, free sites of Au without adsorbed OH are always available, as the maximum OH(ads) coverage on Pt (at 0.85 V) and Au (at 1.3 V) is estimated to be around 0.4-0.5 monolayers.[93] Some researchers believe that glycerol can be oxidized directly to glycerate rather than via glyceraldehyde under alkaline condition,[94] which implies the existence of another reaction pathway.

$$RCH_2OH(ads) + Au - OH(ads) + OH^- \rightarrow Au + RCHO + 2H_2O + e^- \quad (8)$$

$$RCH_2O^-(ads) + Au - OH(ads) \rightarrow Au + RCHO + H_2O + e^- \quad (9)$$

The Au(111), Au(100) and Au(110) surfaces are all reportedly GEOR-active,[95,96] among which Au(111) has the lowest surface energy and highest catalytic activity.[97,98] However, a study comparing the onset potential of OH(ads) formation on (111), (100) and (110) facets of Au showed that Au(110) is the most active one for OH(ads) formation as it has the lowest onset potential of GEOR, followed by (100) and lastly (111).[99]

The fully filled d-band of Au is believed to hinder the bond formation with free radicals of dissociated alcohols, which is one of the explanations of the reduced catalytic activity of Au.[100,101] Nevertheless, this feature prevents both the poisoning effect (CO existing as CO_B[102]) and the

formation of Au-OH(ads).[103] It is noticeable that the poisoning effect reportedly plays a positive role on the efficiency of Au-GEOR (possibly due to the promotion of OH(ads) formation on Au(111) and Au(100) by CO(ads))[104–107]> This is supported by an experiment carried out using SERS to monitor CO(ads) on Au electrode, showing that the onset potential of OH(ads) formation becomes much lower in the presence of CO(ads)[108]. The researchers proposed that the potential of zero charge (PZC) for Au is shifted downward by CO(ads) so that the formation of OH(ads) is promoted.

GEOR on Au is able to highly oxidize glycerol into C1 products, or highly oxidize glycerol into dicarboxylates. Researchers found that Au can adsorb both primary and secondary carbon atoms[77] and it favors C-C bond cleavage towards CO_2 at potentials higher than 0.9 V vs RHE.[36,109,110] The ability to cleave C-C bonds has also been reported by Ottoni et al.[89] using $Pd_{50}Au_{50}$/C, and only C1 products (formate and carbonate) are identified. Similarly, Yongprapat et al.[111] reported a higher selectivity towards formate (>60%) at potentials from 0.2 to 0.4 V vs Hg|HgO. Highly oxidized GEOR products are also commonly identified, which is attributed to a possible mechanism of simultaneous adsorption of either both of the terminal carbon atoms[90] or all three carbon atoms. Oxalate and formate are identified as main oxidation products (>0.95 V vs RHE) by Garcia et al.[91] Tartronate was reported to be produced at a low overpotential (lower than 0.45 V vs RHE)[112] or with a low ratio of glycerol concentration to the surface area, while the secondary hydroxyl group can be oxidized between 0.45 and 0.9 V.[113,114] The reported generation of other products includes DHA and 2,3-dihydroxypropenal, which were produced at 0.39 V vs RHE, whereas glyceraldehyde can be produced at 0.6 V vs RHE, which means that secondary alcohol oxidation is facile at low overpotentials.[115,116] One possible explanation is that Au(100)-OH(ads) favors the deprotonation of secondary carbon atoms.[96]

2.4 Nickel

The demand for new catalysts with lower cost of production has stimulated the development of Ni-based catalysts which exhibit a decent activity compared with noble metals.[7] Fundamental studies have shown that the catalytically active β-NiOOH (generated at 1.3 V vs RHE from β-$Ni(OH)_2$) is responsible for the oxidation of glycerol as well as other alcohols. The mechanism proposed by Fleischmann et al. (also called the indirect electron transfer pathway, see [Eqs. (10) and (11)]) described the oxidation of hydroxyl groups by the reduction of β-NiOOH, which is demonstrated by the observation that no reduction peak appears during the cathodic scan. By contrast, other researchers argue that the alcohol diffuses through the surface and reacts with OH^- on the surface to get oxidized (direct electron transfer pathway).[117,118]

Existing reports show that Ni is capable of cleaving the C-C bond,[9,119] and it is very likely to convert glycerol into C1 products and produce CO_2 (carbonate).[120] Oliveira et al.[9] reported that formate was produced as the major product at 1.6 V vs RHE, while glycolate and glycerate were identified as minor products. Additionally, they also found that switching potentials between 1.6 V and 1.9 V did not strongly affect the selectivity, since glycerate, glycolate and formate were produced in both cases, except the production of CO_2 above 1.70 V.[121] So far, the reaction pathway of C-C bond cleavage (*e.g.* towards to production of formate[9,122]) is still unclear.

$$\beta\text{-NiOOH} + \mathrm{R-CH_2OH} + \mathrm{OH^-} \rightarrow \beta\text{-Ni(OH)}_2 + \mathrm{H_2O} + \mathrm{R-CHO} + \mathrm{e^-} \quad (10)$$

$$\mathrm{R-CHO} + 3\mathrm{OH^-} \rightarrow \mathrm{R-COO^-} + 2\mathrm{H_2O} + 2\mathrm{e^-} \quad (11)$$

In the presence of glycerol, oxygen evolution on NiOOH is shifted to a higher potential,[9] which indicates that NiOOH prefers generating intermediates of GEOR instead of generating OH(ads).[122]

2.5 Summary

In general, many observations with respect to GEOR under various conditions have implied that the oxidation of a primary alcohol group into a primary carboxylate or carboxylic acid is likely to inhibit the oxidation of other alcohol groups.[109] As evidence, the production of glyceraldehyde/glyceric acid and glycolic acid, is favoured over production of tartronic acid, mesoxalic acid and oxalic acid. Also, compared with the easily produced DHA and glyceraldehyde, the production of hydroxypyruvic acid is rarely found, which could be because the oxidation of either a primary alcohol group or a secondary alcohol group would make it more difficult for the oxidation of the remaining group. A second explanation could be the lower possibility of having both terminal carbon atoms and secondary carbon atom simultaneously adsorbed on (111) planes for the oxidation to occur. Similar observations include the one illustrated by Miller et al.[78] that diols with two alcohol groups on adjacent carbon atoms tend to be oxidized into mono-carboxylates, while diols without this adjacency can be oxidized into di-carboxylates or ketones.

3 General Discussion

Detailed analysis of the reaction mechanisms of GEOR is always hindered by the uncertain interpretations of observed results. This issue is worsened by vaguely using words such as "favor" and "improve", because in some cases these words describe the efficiency of GEOR reactions, and in other cases they mean a higher selectivity towards certain products. Many of the controversies might have been resolved if the exact meaning of these descriptions were given.

Since the 1990s, *in-situ* FTIR has been used for monitoring electrochemical interfaces.[123] In the last decade, this method has been applied to the identification of the adsorbates and intermediates during GEOR. So far, many peaks / bands of IR spectra have been assigned to specific vibrational modes.[50,124] Nevertheless, controversies of peak identification still exist as the convolution of peaks may mask weak bands or shift the center of peaks. Overall, several facts can be confirmed by interpreting IR spectroscopic results.

In many GEOR studies by FTIR, Pt and Pd electrodes show three "stages" (denoted as **Stage I, II and III** here) as the overpotential is increased.[33,57,61,64] Initially in Stage I, at low overpotentials which do not facilitate the formation of OH(ads), a complete decomposition of glycerol can occur, which is confirmed by characteristic peaks of CO_L (mostly at Pt(111) and Pt(110)) and CO_B (mostly at Pd and Pt(100)) (see Figure 4a-4c), together with the parallel production of glyceraldehyde.[58] Another proof of complete dissociation is that an experiment using isotope-labelled terminal carbon atoms show that CO(ads) are generated from both terminal and secondary carbon atoms (see Figure 4d).[57] When the potential is above approximately 0.6 V into Stage II, the bands of CO(ads) disappear (see Figure 4e), shrink or remain unchanged (rarely seen), indicating that the amount of CO adsorbed on the surfaces of Pt and Pd stop increasing.[58] Meanwhile, carboxylates are rapidly produced and accumulate, as revealed by the complexity of spectra in the range of 1100-1600 cm^{-1}. The beginning of the last stage is characterized by a steeply rising peak at 2343-2345 cm^{-1} (usually above 1.0-1.1 V vs RHE), which translates into the evolution of CO_2. At the same time, the peaks of carboxylates stop rising. The staging demonstrated in this paragraph can be clearly indicated by the change in the IR intensities of CO(ads) and CO_2 (see Figure 4e).

Au is a special case as it very rarely produces CO(ads), and therefore CO_2 production is also limited (even though a short peak at 2343 cm^{-1} can be seen for some cases). Carboxylate peaks are usually seen, and are the only features in the FTIR spectra for Au.[77,91]

It is believed by many researchers that the capacity of Pd to cleave C-C bonds of glycerol is weaker than Pt (referred to here as **Proposition A**).[25] This proposition is usually supported by two empirical observations: (1) a larger portion of C3 intermediates is often reported from Pd

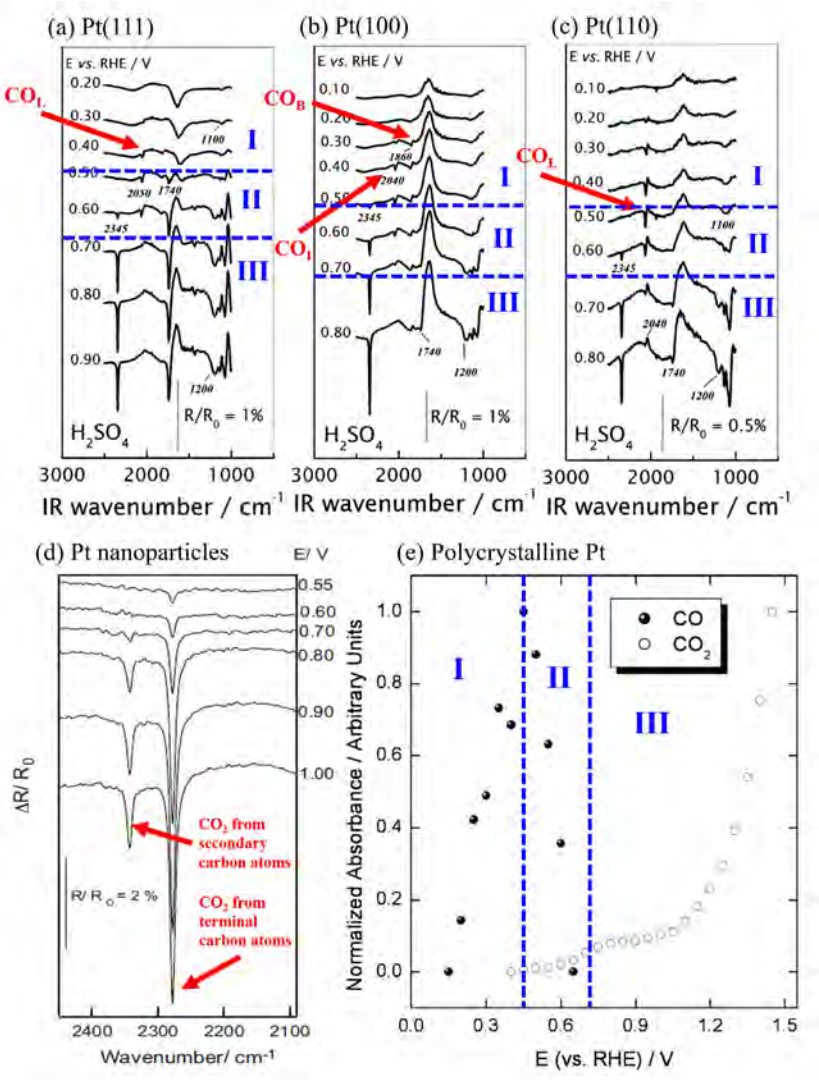

Figure 4: *In-Situ* FTIR spectra of glycerol electrooxdation with Pt catalysts and the analyses of adsorbed CO on Pt. (a-c) *In-situ* FTIR spectra of GEOR on Pt monocrystalline in 0.1 M glycerol with 0.1 M $HClO_4$ or H_2SO_4. (Reprinted with permission from Ref[61], with annotations in red and blue. Copyright © 2012 Elsevier Ltd. All rights reserved.) (d) *In-situ* FTIR spectra in the presence of 0.255 M $^{13}CH_2OH$–$^{12}CHOH$–$^{13}CH_2OH$ + 0.1 M $HClO_4$. (Reprinted with permission from Ref[57], with annotations in red. Copyright © 2012 Elsevier Ltd. All rights reserved.) (e) Normalized absorbance of CO and CO_2 for GEOR at different potentials (0.1 M glycerol with 0.1 M $HClO_4$) (Reprinted with permission from Ref[58], with annotations in blue. Copyright © 2011 Elsevier Ltd. All rights reserved.)

Table 1: Reported onset potentials of GEOR, OH adsorption, and surface oxide formation with Pt and Pd electrodes. Potentials vs RHE unless otherwise stated

	Onset Potentials	
	Pt	Pd
GEOR	0.05 V for (110),(100) [30]	0.4 V [64], 0.6 V [74]
OH(ads)	0.4 V [59], 0.5-0.6 V [20]	0.15 V vs HgO [129]
Oxide	0.5 V [93]	0.5 V [130], 0.67 V [131], 0.7 V [74]

catalysts than Pt,[46] and (2) the current density of Pd obtained in cyclic voltammetry is much lower than Pt (see Figure 5a).[29] In fact, this conclusion is doubtful, as there are many spectra comparing Pt and Pd catalysts showing that the onset potentials at which CO(ads) is formed on the surface of Pt and Pd are very close (see Figure 5b-5c), and both Pt and Pd can catalyze glycerol oxidation to produce large amounts of CO_2 at high potentials in Stage III (see Figure 6).[50,59,62,64,125,126] Comparative DFT studies are strongly needed to justify this proposition. DFT studies conducted by Rangarajan et al.[127] investigated the energetically favored reaction pathways of GEOR at Pt and Pd electrodes and found that both Pt and Pd favor C-C bond scission (after three deprotonation steps) over C-O bond scission, which matches what was found by Greeley et al.[41]. Liu and Greeley[128] also revealed that the decomposition energetics of glycerol on Pd (111) and Pt (111) are similar, with Pd (111) having a higher C-C scission transition state energy.

Proposition A becomes clearer if it is combined with three other observations: (1) higher overpotentials and alkaline electrolytes lower the cleavability of C-C bonds on Pt,[16,36] whereas they improve the C-C bond dissociation on Pd.[74,76,77] (2) GEOR occurring on the surface of Pd is usually in alkaline conditions as its activity (current density) is very limited in acidic solutions compared with Pt.[15] (3) The difference between the onset potentials of rapid GEOR and OH(ads) formation are much closer in the cases of Pd than Pt (see Table 1).

Based on these three widely reported observations, it is important to re-visit **Proposition A**, as researchers tend to use this proposition but not to consider the effect of OH(ads) on deprotonation in different stages. In Stage I, the dissociative adsorption of glycerol on Pd is very slow, and only a few researchers detected CO(ads) signals at low overpotentials (*e.g.* 0.3 V vs RHE) where there is no OH adsorption. Under circumstances where OH(ads) is generated and promotes the dissociative adsorption of glycerol, Pd catalysts share a similar selectivity towards C2/C1 products with Pt. Higher overpotentials and alkalinity of electrolytes can bring both Pd and Pt to a stage where OH(ads) acts as a major reactant with glycerol. On one hand, as illustrated by [Eq. (5)], OH(ads) is able to convert poisoning species CO(ads) into CO_2 via a Langmuir-Hinshelwood mechanism. On the other hand, glyceric acid, glycolic and formic acid can be produced via the production of carboxylates [Eq. (7)], which means that a large portion of oxidized glycerol is directed to carboxylate (mainly glycerate[40,58,132,133]), rather than completely oxidized into CO(ads). As the current density under such circumstances is much higher than for low-overpotential / acidic conditions, aside from the production of carboxylates which are represented by multiple IR bands overlapping each other, many researchers report increasing generation of CO_2 due to the fast depletion of OH^- at the working electrode, while others find an increase of the IR band of carbonate (exemplified by Lima et al.[37] and deSouza et al.[134]). Therefore, "selectivity" can be hard to determine as it is very challenging to quantify the IR bands of different products and intermediates measured in real time. When referring to **Proposition A**, researchers are strongly encouraged to clarify the experimental conditions, and emphasize whether they mean the selectivity of GEOR towards C1/C2 or C3 products.

As the potential increases from Stage II to Stage III, the peak intensities of carboxylates basically remain unchanged after rapidly rising in the beginning of Stage II (in both acidic and alkaline

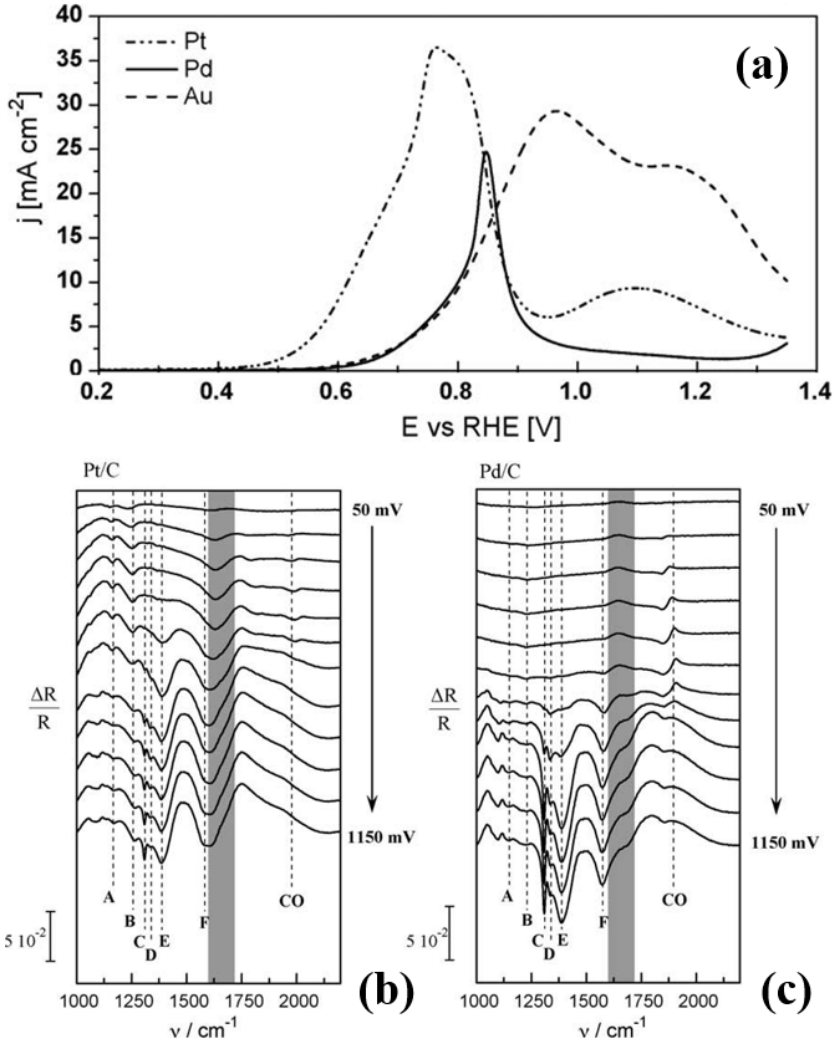

Figure 5: Cyclic voltammograms and *In-Situ* FTIR spectra and of glycerol electrooxidation with Pt and Pd electrocatalysts. (a) Cyclic voltammetry showing GEOR with Pt, Pd, and Au at room temperature (0.1 M glycerol + 1.0 M NaOH electrolyte). (b-c) *In-situ* infrared spectra of GEOR with Pt/C and Pd/C working electrodes (Reprinted with permission from Ref[29], Copyright © 2009 Elsevier B.V. All rights reserved.).

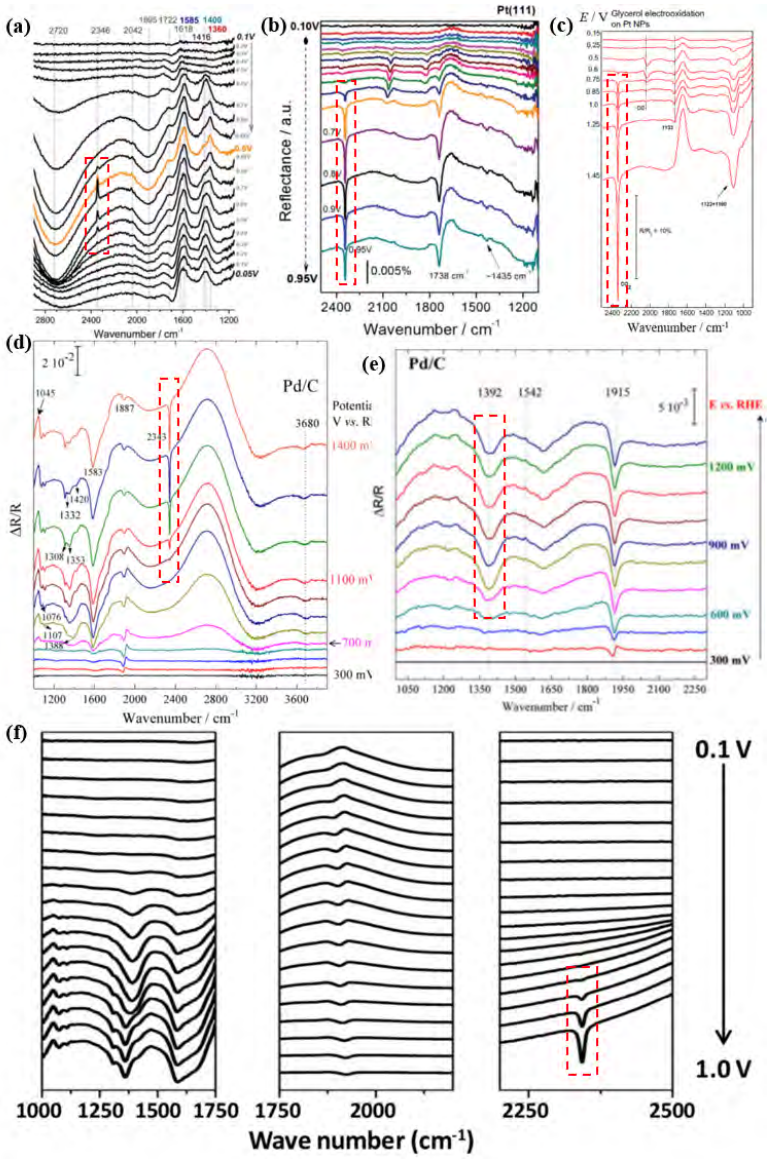

Figure 6: *In-situ* FTIR potential-dependent spectra of GEOR with Pt and Pd catalysts. (a) 0.5 M glycerol in 0.1 M NaOH on Pt(111). Potential: 0.05 to 0.9 V; (Reprinted with permission from Ref[62], © 2017 Elsevier B.V. All rights reserved.) (b) 0.2 M glycerol in 0.5 M H_2SO_4 solution with Pt(111) (Reprinted with permission from Ref[59], © the Owner Societies 2016) (c) 0.05 M glycerol & 0.1 M $HClO_4$ with Pt nanoparticles (Reprinted with permission from Ref[125], Copyright © 2014 Elsevier B.V.) (d) 0.1 M glycerol in 0.1 M NaOH electrolyte at 1 mV s^{-1} on Pd/C (Reprinted with permission from Ref[64], Copyright © 2013 American Chemical Society) (e) 0.1 M glycerol in 0.1 M NaOH on Pd/C (Reprinted with permission from Ref[126], © Springer Science+Business Media New York 2013) (f) 0.1 M glycerol in 0.1 M NaOH at Pd. Scan rate: 1 mV s^{-1} (Reprinted with permission from Ref[50], Copyright © 2015 Elsevier Ltd. All rights reserved.) IR bands of CO_2 (2343 cm^{-1}) or carbonate (1398 cm^{-1}) are highlighted by dashed rectangles in red.

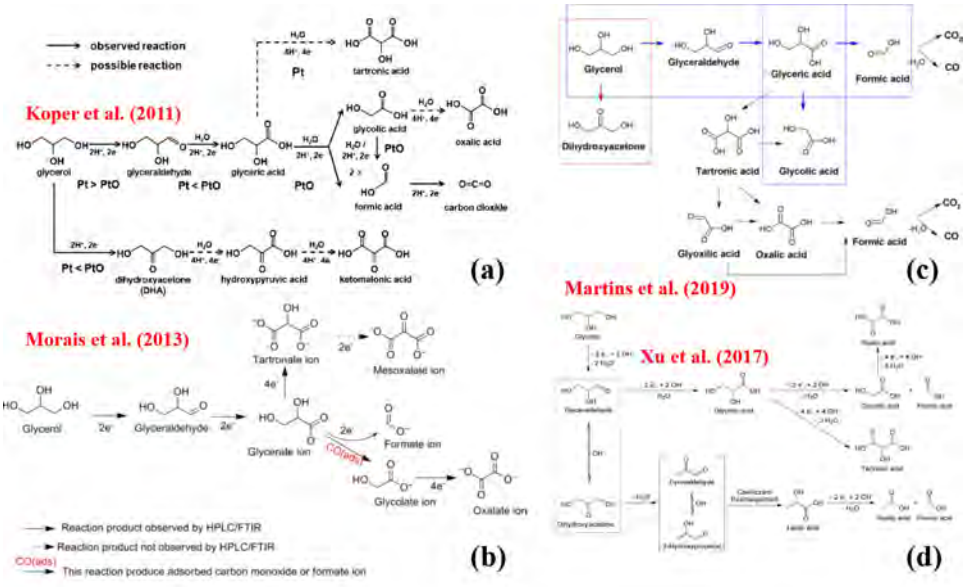

Figure 7: Previously reported reaction pathways of glycerol electrooxidation. (a) The glycerol oxidation mechanism on a Pt electrode in acidic media. (Reprinted with permission from Ref[30], Copyright © 2011 WILEY-VCH Verlag GmbH & Co. KGaA, Weinheim) (b) Proposed reaction scheme for glycerol electrooxidation on PdNi/C and PdAg/C nanocatalysts in alkaline medium. (Reprinted with permission from Ref[64], Copyright © 2013 American Chemical Society) (c) Schematic suggested pathways for glycerol electrooxidation on Pt surfaces in acid medium (Reprinted with permission from Ref[17], © Springer Science+Business Media, LLC, part of Springer Nature 2018) (d) Proposed reaction pathways for glycerol oxidation in alkaline solution on AuPt catalysts. (Reprinted with permission from Ref[36], © 2017 Elsevier Inc. All rights reserved.)

conditions), while evolution of CO_2 becomes a major feature. Another proposition proposed by researchers (**Proposition B**) is that the massive production of CO_2 in Stage III (usually above 1.0-1.1 V vs RHE) is due to the electrooxidation of carboxylate intermediates. In almost all GEOR studies reporting the generation of CO_2 or carbonate, they are produced from the oxidation of formic acid / formate (which is produced from the oxidation of other C2/C3 intermediates). However, there are several GEOR studies proposing the production of CO_2 / carbonate directly from glycolic acid / glycolate,[84,135] oxalic acid / oxalate[114,132], and tartronic acid / tartronate[50,56]. This proposition is usually developed into a reaction mechanism that attributes the production of C1/C2 products to the electrooxidation of C2/C3 intermediates (see Figure 7).[17,30,36,64] A cautious verification of Proposition B requires two aspects: (1) showing that these C3/C2 intermediates have a relatively higher probability to be further oxidized than glycerol, and (2) how CO_2 / formate / C2 intermediates are produced at high overpotentials in Stage II and Stage III.

Exemplified by a Pd and a PdAg electrodes, at a constant potential (*e.g.* 0.8 V vs RHE[64]) where there is no CO_2 production observed, the peak intensities of carboxylates increase versus time, but the ratio of the intensities remains the same (see Figure 8a-8b). Also, the HPLC results displayed in Figure 8c-d[36] shows that the percentage of each side product remains the same throughout the electrooxidation, showing that no significant amount of any side product is further oxidized into

other side products. Similarly, as shown in Figure 8d (PtFe composites oxidizing glycerol towards tartronic acid under alkaline conditions[136]), the rapid conversion from glycerate into tartronate and other side products occurs only after the complete depletion of glycerol. This strongly supports the fact that C3 intermediates can be oxidized into other highly oxidized products, but only in the absence of glycerol. Also, Koper et al.[33] compared the current densities of oxidizing glycerol, glyceraldehyde and DHA using Pt(111) and Pt(100) under acidic conditions. The results (Figure 8e) reveal that the current densities of glyceraldehyde and DHA oxidation are approximately one order of magnitude smaller than the current density of GEOR, which indicates that glycerol has higher reactivity than glyceraldehyde and DHA. (Very few researchers have ever reported C-C bond cleavage of tartronic acid and mesoxalic acid. Also, no studies have compared the current densities of C2 intermediates with that of glycerol.) Considering the massive production of CO_2 monitored by *in-situ* FTIR, it is unlikely that the majority of CO_2 originates from intermediates (except from formic acid / formate), as they are outnumbered by glycerol. In those GEOR studies in which formate was reported as a major side product, the portion of CO_2 production directly from glycerol (through CO(ads), which is produced from the full dissociation of glycerol) or from the oxidation of formate needs to be carefully assessed before proposing reaction pathways.

Generally, the rapid generation of CO_2 at higher overpotentials is regarded as a sign that the cleavage of C-C bonds is accelerated at such potentials. However, inspecting the spectra (Figure 9a-9b) obtained by Camara et al.[130] at PdRh electrodes, the peak at 1574 cm^{-1} (carboxylate) kept rising (although slowly) as the potential increased from 0.63 V to 1.3 V when 1 M KOH was used to better maintain the pH of the electrolyte at the interface. This observation shows that the levelling off of peak intensities of carboxylates at potentials above which the signal of CO_2 is detected is due to the complete consumption of hydroxide in the interface region, rather than the higher overpotentials favoring (a higher selectivity) C-C bond cleavage of glycerol and C3 intermediates. However, since the complete oxidation of glycerol into carbonate consumes 20 hydroxide ions per molecule of glycerol, the alkalinity of the electrolyte cannot be easily maintained if the applied potential facilitates a fast oxidation. It is also observed that the peak of CO(ads) vanishes at different potentials (or not at all throughout the whole potential range) in various studies.[57,58] A widely accepted explanation is that the band intensity of CO(ads) depends on the rate of its generation and consumption,[58] thereby a fast consumption of CO(ads) would lead to an earlier disappearance of the CO(ads) peak. In acidic conditions, only Pt(100) exhibits more C-C bond cleavage in Stage II and conversion into CO_2 (see Figure 4b).[61]

Based on the explanation given in the above paragraphs, Proposition B is unlikely to be true. Combining both propositions that are discussed in this section, a full picture of GEOR with Pt and Pd catalysts can now be presented. It is most likely that C3/C2/C1 "intermediates" (or side products) of GEOR are generated from both resources, that is, directly generated from glycerol (mainstream) and indirectly generated from intermediates that are lightly oxidized (minor). The overpotentials and the alkalinity of the electrolytes are the most important factors controlling the portion of each. Therefore, a new reaction mechanism that differs from previously presented reaction pathways (exemplified by reaction pathways shown in Figure 7a-d) is proposed in Section 4.

4 Parallel Pathways Proposed as the Major Reaction Mechanism of Glycerol Electrooxidation

Recent GEOR studies have proposed many reaction pathways and mechanisms, contributed by, among others, the groups of Koper[30,33,34], Coutanceau[55,74,137], Fernández[37,38,42,134] and Martins[17,84,138]. Soluble intermediates and products are well established by experiment, but evidence for surface-adsorbed intermediates comes mainly from DFT studies. Overall, a well-established

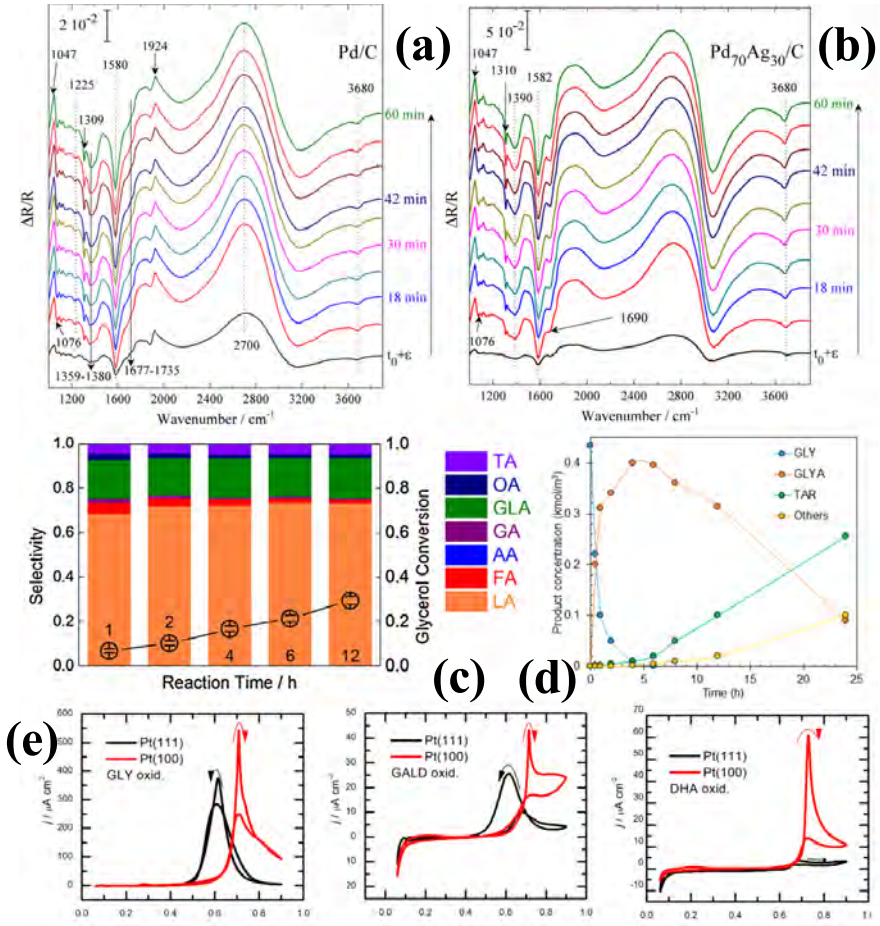

Figure 8: *In-situ* FTIR spectra, HPLC results and cyclic voltammograms showing the results of glycerol electrooxidation with various electrocatalysts. (a-b) FTIR spectra recorded during chronoamperometry in 0.1 M NaOH + 0.1 M glycerol on Pd/C and $Pd_{70}Ag_{30}$/C catalysts at 0.8 V vs RHE. (Reprinted with permission from Ref[64], Copyright © 2013 American Chemical Society) (c) AuPt (15% Pt_{surf}) with applied potential of 0.45 V vs RHE in 0.5 M glycerol & 1 M KOH solution in 12 h. (Reprinted with permission from Ref[36], © 2017 Elsevier Inc. All rights reserved.) (d) concentration-time profiles on the annealed $PtFe_{4.5}$ catalyst (GLY: glycerol, GLYA: glyceric acid, TAR: tartronic acid, Others: lactic acid, formic acid, etc) in 0.43 M glycerol + 1.2 M KOH solution (Reprinted with permission from Ref[136], Copyright © 2017 American Chemical Society) (e) Cyclic voltammograms for 0.1 M of glycerol, glyceraldehyde, and DHA oxidation on Pt(111) (black line) and Pt(100) (red line) electrodes in $HClO_4$, respectively. (Reprinted with permission from Ref[33], Copyright © 2016 American Chemical Society)

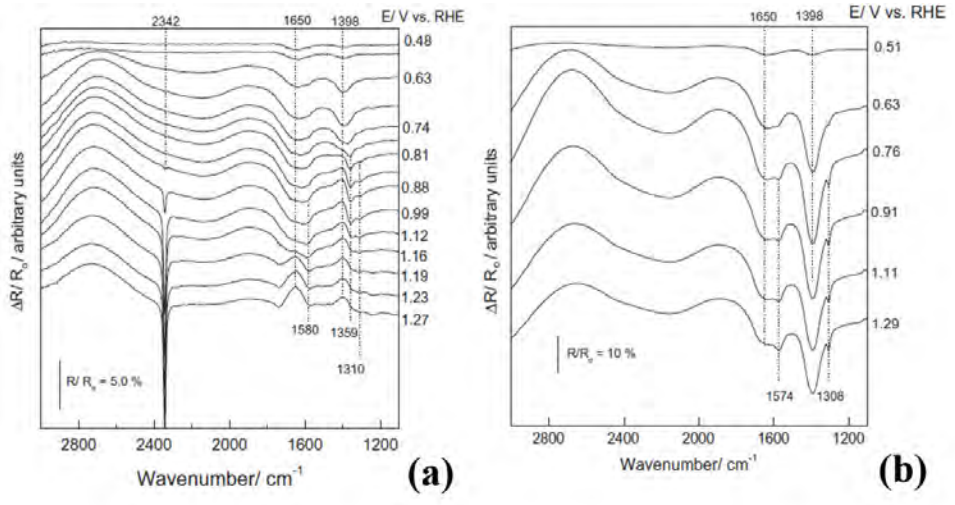

Figure 9: *In-situ* FTIR spectra in (a) 0.1 M and (b) 1.0 M KOH + 0.1 M glycerol on PdRh. (Reprinted with permission from Ref[130], © 2013 Elsevier B.V. All rights reserved.)

mechanism of GEOR in terms of individual reaction steps has not yet been presented. Based on the experimental results from many GEOR studies, an approach to illustrate the reaction mechanism through the initial dissociative adsorption of carbon atom which interpretes the behavior of Pt, Pd and Au is proposed below, which awaits reliable experimental results for full validation. It explains how a high selectivity towards C-C bond cleavage, glycerate, or DHA is achieved, and also explains many common observations and hypotheses. It should be noticed that as C-adsorbates are more stable than O-adsorbates, the reaction pathways that involve O-adsorbates are not mentioned here. Also, as GEOR through C-adsorption involves many pathways which may co-exist during the reaction, in this section we focus on the major pathways that lead to full dissociation and production of carboxylates.

4.1 Dual Pathways of Deprotonation Processes on Pt, Pd, and Au

Different from the model shown in Figure 10a presented by Camara et al.[57], DFT studies[33,115,132,139–141] have shown that glycerol molecules can contact the (111) facet of Pt, Pd, and Au through carbon atom and / or oxygen atom (as shown in Figure 10b-d). However, the C-adsorption pathway is more involved in C-C bond cleavage, as M-CO(ads) is commonly seen in GEOR, and has been widely accepted as the main poisoning species generated from the C-adsorption pathway for the electrooxidation of methanol, and formic acid.

It has been clearly and extensively proven that Pt(111), Pt(100) and Pt(110) are able to catalytically oxidize glycerol in acidic solutions at potentials which cannot generate OH(ads) (*e.g.* below 0.5 V vs RHE).[57,58,61] This complete oxidation of glycerol triggers the widely recognized poisoning effect caused by adsorbed species. This observation indicates that base catalysis is not the only way through which O-H cleavage and dehydrogenation can occur. Instead, it is more likely to be one of several possible ways. In acidic conditions, on Pt(100), Pt(110) and Pt(111) facets, both primary and secondary alcohols may oxidize through [Eqs. (12)-(17)] or [Eqs. (18)-(19)]. Please

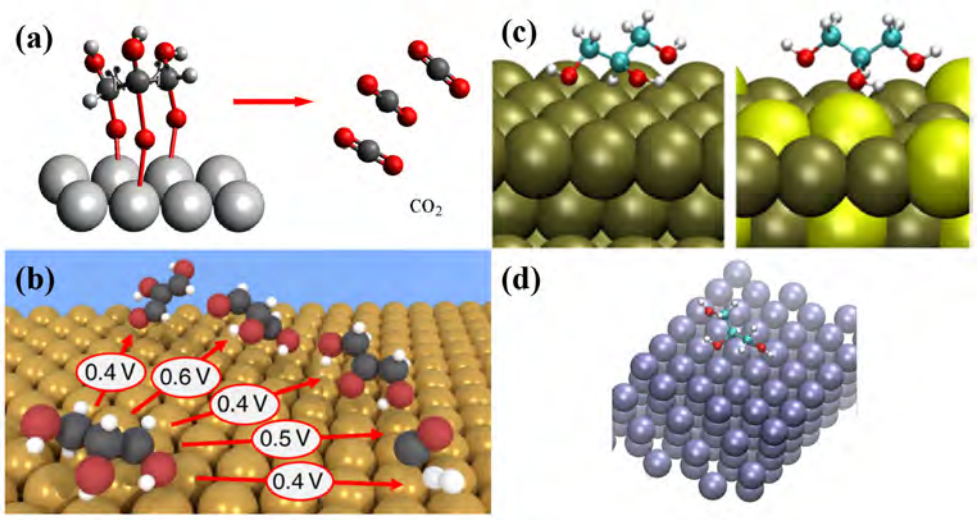

Figure 10: Schematic illustration and DFT studies of GEOR on various metallic electrocatalysts. (a) Schematic illustration of GEOR on Pt nanoparticles towards the production of CO_2 (reprinted with permission from Ref[57], Copyright © 2012 Elsevier Ltd. All rights reserved.). (b) Schematic illustration of DFT results of GEOR on gold in alkaline medium (reprinted with permission from Ref[115], Copyright © 2018 American Chemical Society). (c) Glycerol adsorbed on Pd(111) (left) and $Pd_{0.77}Pb_{0.23}$(111) (right) using DFT calculations (reprinted with permission from Ref[139], © Springer Science+Business Media, LLC, part of Springer Nature 2018). (d) Schematic illustration of DFT results of glycerol binding on Pt in acidic medium (reprinted with permission from Ref[132], © 2017 Wiley-VCH Verlag GmbH & Co. KGaA, Weinheim).

be reminded that as proposed by Koper et al., the second deprotonation may occur initially on carbon atom, but a proton can be transferred to the primary carbon atom from the primary OH group.[33] The partial deprotonation at a primary carbon produces glyceraldehyde and deprotonation at the secondary carbon leads to DHA.[33] In addition, complete deprotonation at a primary carbon generates $CH_2OHCHOHCO(ads)$,[142] which is an intermediate leading to C-C bond cleavage. This cleavage is shown by the production of CO(ads) in acidic conditions and the subsequent evolution of CO_2. This pathway from glycerol to glyceraldehyde, DHA and CO(ads) is called here the **acidic (OH-free) pathway** (asterisks indicate C atoms bonded to the surface; two asterisks mean bonding to two metal atoms):

Acidic pathway:

$$\text{site} + CH_2OHCH(OH)CH_2OH \rightarrow CH_2OHCH(OH)\mathbf{C}^*HOH(ads) + H^+ + e^- \quad (12)$$

$$CH_2OHCH(OH)\mathbf{C}^*HOH(ads) \rightarrow CH_2OHCH(OH)\mathbf{C}^*OH(ads) + H^+ + e^- \text{ (metal=C double bond)} \quad (13)$$

$$\text{Or } CH_2OHCH(OH)\mathbf{C}^*HOH(ads) \rightarrow CH_2OHCH(OH)\mathbf{C}^*HO(ads) + H^+ + e^- \quad (14)$$

$$CH_2OHCH(OH)\mathbf{C}^*OH(ads) + \text{site} \rightarrow CH_2OHCH(OH)\mathbf{C}^{**}O(ads) + H^+ + e^- \quad (15)$$

$$\text{Or } CH_2OHCH(OH)\mathbf{C}^*HO(ads) + \text{site} \rightarrow CH_2OHCH(OH)\mathbf{C}^{**}O(ads) + H^+ + e^- \quad (16)$$

$$CH_2OHCH(OH)\mathbf{C}^{**}O(ads) \rightarrow CH_2OHCH(OH)\mathbf{C}^*O(ads) + \text{site} \quad (17)$$

$$\text{site} + CH_2OHCH(OH)CH_2OH \rightarrow CH_2OH\mathbf{C}^*(OH)CH_2OH(ads) + H^+ + e^- \quad (18)$$

$$CH_2OH\mathbf{C}^*(OH)CH_2OH(ads) \rightarrow \text{site} + \text{ dihydroxyacetone } + H^+ + e^- \quad (19)$$

Reaction mechanisms differ significantly when OH^- is present under alkaline condition or at high overpotentials in an acidic solution. Pt-OH(ads), which is produced via Eq. (20) and Eq. (21) in basic and acidic solution, respectively, promotes the deprotonation of glycerol. From Eq. (22) to Eq. (27), $CH_2OHCHOHCO(ads)$ can also form on the Pt surface. (Eqs.(22)-(24) show the production of $CH_2OHCHOHCO(ads)$ in acidic condition at high overpotentials, while the production of $CH_2OHCHOHCO(ads)$ in strong base is displayed as Eqs. (25)-(27)) However, instead of removing this adsorbate through C-C bond cleavage, a reaction between $CH_2OHCHOHCO(ads)$ and OH(ads) can occur rapidly to convert this intermediate into glyceric acid / glycerate (Eq. (29)), followed by its desorption. Behm et al.[60] has shown that in the potential range of 0.6-0.7 V, over 95% of the current goes to incomplete oxidation of glycerol. Presumably, this **OH(ads)-present pathway** tends to oxidize glycerol all the way to glyceric acid while also producing glyceraldehyde and DHA (Eqs. (30)-(31)).

OH(ads)-present pathway:

$$OH^- \rightarrow OH(ads) + e^- \quad (20)$$

$$\text{site} + H_2O \rightarrow OH(ads) + H^+ + e^- \quad (21)$$

$$OH(ads) + CH_2OHCH(OH)CH_2OH \rightarrow CH_2OHCH(OH)\mathbf{C}^*HOH(ads) + H_2O \quad (22)$$

$$CH_2OHCH(OH)\mathbf{C}^*HOH(ads) + OH(ads) \rightarrow CH_2OHCH(OH)\mathbf{C}^*HO(ads) + \text{site} + H_2O \quad (23)$$

$$CH_2OHCH(OH)\mathbf{C}^*HO(ads) + OH(ads) \rightarrow CH_2OHCH(OH)\mathbf{C}^{**}O(ads) + H_2O \quad (24)$$

$$OH^- + CH_2OHCH(OH)CH_2OH \rightarrow CH_2OHCH(OH)CH_2O^- + H_2O \quad (25)$$

$$CH_2OHCH(OH)CH_2O^- + OH(ads) \rightarrow CH_2OHCH(OH)\mathbf{C}^*HO^-(ads) + H_2O \quad (26)$$

$$CH_2OHCH(OH)\mathbf{C}^*HO^-(ads) + OH(ads) \rightarrow CH_2OHCH(OH)\mathbf{C}^{**}O(ads) + H_2O + e^- \quad (27)$$

$$CH_2OHCH(OH)\mathbf{C}^{**}O(ads) \rightarrow CH_2OHCH(OH)\mathbf{C}^*O(ads) + site \quad (28)$$

$$CH_2OHCH(OH)\mathbf{C}^*O(ads) + OH(ads) \rightarrow CH_2OHCH(OH)\mathbf{C}^*OOH(ads) + site \quad (29)$$

$$OH(ads) + CH_2OHCH(OH)CH_2OH \rightarrow CH_2OH\mathbf{C}^*(OH)CH_2OH(ads) + H_2O \quad (30)$$

$$CH_2OH\mathbf{C}^*(OH)CH_2OH(ads) + OH(ads) \rightarrow 2M + \text{dihroxyacetone} + H_2O \quad (31)$$

However, the generation of glyceraldehyde as a final product can be suppressed as glyceraldehyde deprotonates again by reacting with OH(ads) to give $CH_2OHCHOHCO(ads)$ via an Eley-Rideal mechanism.[57] Given the observation that the removal of CO(ads) with OH(ads) is the rate-determining step, the deprotonation steps are faster, which leads to a higher rate of $CH_2OHCHOHCOOH(ads)$ and $CH_2OHCOCH_2OH(ads)$ generation. Also, this interpretation successfully matches the mainstream observations that C-C cleavage is favored in acidic solution and at low overpotentials in Stage I. One good example for GEOR in acidic condition was presented by Melle et al.[143], showing that glyceraldehyde has a tendency to be quickly deprontonated and cleaved at polycrystalline Pt at overpotentials lower than 0.8 V, producing CO(ads) to poison the surface. The absence of glyceric acid at such low potentials is because the pathway towards $CH_2OHCHOHCOOH(ads)$ competing with the pathway of C-C bond cleavage does not exist under these conditions.

According to many GEOR studies, Pd has a much higher d-band center and lower catalytic activity compared to Pt.[32] Also, it is observed that the catalytic activity of Pd is much inferior to Pt without base-catalyzed deprotonations.[142] In addition, from cyclic voltammetry under alkaline condition, the onset potential of observable GEOR is very close to the formation of OH(ads) (*e.g.* within 100 mV) (see Table 1). These correlated results translate into a hypothesis that the acidic pathway does exist in the case of Pd but is very limited.[70] Instead, the OH(ads)-present pathway is definitely the main pathway for GEOR occurring on Pd, supported by the fact that very few GEOR studies with Pd were conducted under acidic condition. This proposition perfectly explains the positive role OH^- plays in Pd catalysts in cleaving C-C bonds, because the formation of Pd-$CH_2OHCHOHCO(ads)$ can only be promoted by OH^- through the OH(ads)-present pathway, in contrast to its negative impacts in the case of Pt.

With the addition of adatoms like Bi and Sb, two observations are usually obtained with Pd and Pt catalysts, that is, higher selectivity towards DHA and reduced ability to dissociate C-C bonds (detailed in Section 5). Researchers have presented the theory that oxidation through a primary carbon relies on the presence of three adjacent Pt(111)/Pd(111) sites, and the introduction of Bi can disturb this vicinity and thus disable this pathway. This explanation is consistent with the mechanism proposed here, as the reduced number of vicinal Pt/Pd atoms affects both acidic and OH-present pathways towards $CH_2OHCHOHCO(ads)$, and therefore the intermediates (glyceraldehyde, glyceric acid, C1/C2 products) produced via these processes are suppressed.

Distinct from Pt and Pd, Au shows no catalytic activity through the acidic pathway as the vast majority of researchers reported. This is supported by the fact that the onset potential of GEOR matches the onset potential of Au-OH(ads) formation under alkaline conditions.[87,91,144] Compared with bare Au, Au-OH(ads) has a much higher ability to break C-H bonds and O-H bonds, and therefore a high activity of GEOR (large current density) is commonly reported.[86] $CH_2OHCHOHCO(ads)$ on the surface of Au(111) can be converted very easily into C1/C2 products,[91] which is possibly due to the lowest d-band center among the three noble metals (-3.56 eV)[32] destabilizing RCO(ads). Besides, it has been widely reported that CO(ads) can further lower the d-band center of Au (*e.g.* 3 eV for Au monomer[145]), as the 5d bands narrows and the number of states reduces near E_F(Fermi level), which implies a promoting effect of CO(ads) on the catalytic activity of Au. A lower d-band center would increase the filling of the anti-bonding orbital

of the adsorbed molecule and therefore facilitates the dissociation. The inexistence of the acidic pathway may be a result of a surface covered by sulfate / perchlorate in acidic solution, disabling the oxidation of glycerol.[115]

4.2 Cleavage of C-C Bonds and Selectivity towards C1/C2 Products

The mechanism of dissociation of C-C bonds of $CH_2OHCHOHCO$(ads) on the surface of metals still remains unclear as there are few mechanistic studies. However, it is clear that the further reaction of $CH_2OHCHOHC^*O$(ads) has two directions, either through a cleaved C-C bond, or through the reaction with OH(ads) to give glyceric acid / glycerate (as illustrated above in Eq. (29) and below in Eq. (32)). Considering that glycerol can be adsorbed onto Pt(100) with only one terminal carbon atom adsorbed and still generate CO(ads),[33] two Pt-C chemisorption bonds are presumably not a prerequisite for C-C bond cleavage. According to the previously reported reaction mechanism of ethanol and propanol electrooxidation with respect to bond cleavage ($CH_3CO(ads) \rightarrow CH_3(ads) + CO(ads), CH_3CH_2CO(ads) \rightarrow CH_3CH_2(ads) + CO(ads)$),[22] poly-ols with adjacent hydroxyl groups should have a much better reactivity as the newly adsorbed species bear hydroxyl groups for further deprotonation and bond cleavage. Please note that after deprotonation steps (Eq.(33)), the C-C bond dissociation proposed here (Eq. (34)) does not involve OH(ads) and electron transfer. As a result of this cleavage, a poisoning species (CO(ads) or CO_B(ads)) is formed, together with the generation of a new and shorter adsorbate with one fewer carbon (*i.e.* CH_2OHCO(ads)), waiting for conversion into glycolic acid (Eq. (35)). Under this circumstance, after deprotonation (Eq. (36)), C-C bond cleavage may occur the second time (see Eq. (37)), generating more CO(ads) and C1 intermediates. It is clearly shown in many studies on methanol electrooxidation at Pt that C1 intermediates can either be reacted into formic acid (Eqs. (38)) or deprotonated and left on the surface as the poisoning species CO(ads) (Eq. (39)).

GEOR to various products:

$$CH_2OHCHOH\mathbf{C}^*O(ads) + OH(ads) \rightarrow CH_2OHCHOH\mathbf{C}^*OOH(ads) + M \quad (32)$$

$$CH_2OHCHOH\mathbf{C}^*O(ads) + site \rightarrow CH_2OH\mathbf{C}^*O\mathbf{C}^*O(ads) + 2H^+ + 2e^- \quad (33)$$

$$\text{Or } CH_2OHCHOH\mathbf{C}^*O(ads) + 2\ OH(ads) \rightarrow CH_2OH\mathbf{C}^*O\mathbf{C}^*O(ads) + 2H_2O + site$$

$$CH_2OH\mathbf{C}^*O\mathbf{C}^*O(ads) \rightarrow CH_2OH\mathbf{C}^*O(ads) + CO(ads) \quad (34)$$

$$\text{Or } CH_2OH\mathbf{C}^*O\mathbf{C}^*O(ads) + site \rightarrow CH_2OH\mathbf{C}^*O(ads) + CO(ads)(CO_B)$$

$$CH_2OH\mathbf{C}^*O(ads) + OH(ads) \rightarrow CH_2OH\mathbf{C}^*OOH(ads)\ \text{(glycolic acid)} \quad (35)$$

$$CH_2OH\mathbf{C}^*O(ads) + site \rightarrow \mathbf{C}^*HO\mathbf{C}^*O(ads) + 2H^+ + 2e^- \quad (36)$$

$$\text{Or } CH_2OH\mathbf{C}^*O(ads) + 2\ OH(ads) \rightarrow \mathbf{C}^*HO\mathbf{C}^*O(ads) + 2H_2O + site$$

$$\mathbf{C}^*HO\mathbf{C}^*O(ads) \rightarrow H\mathbf{C}^*O(ads) + \mathbf{C}O(ads) \quad (37)$$

$$\text{Or } \mathbf{C}^*HO\mathbf{C}^*O(ads) + site \rightarrow H\mathbf{C}^*O(ads) + \mathbf{C}O(ads)(CO_B)$$

$$H\mathbf{C}^*O(ads) + OH(ads) \rightarrow H\mathbf{C}OOH(ads)\ \text{(formic acid)} + site \quad (38)$$

$$H\mathbf{C}^*O(ads) \rightarrow \mathbf{C}O(ads) + H^+ + e^- \quad (39)$$

$$\text{Or } H\mathbf{C}^*O(ads) + site \rightarrow \mathbf{C}O(ads)(CO_B) + H^+ + e^-$$

In summary, it is hypothesized that the $R^{(n)}CO$(ads) intermediates, can react in two ways: either reacting with OH(ads) to **monocarboxylic acid / monocarboxylate**, or degrading to $\mathbf{R}^{(n-1)}\mathbf{CO}$(ads) until they are fully oxidized to C1 products and intermediates (*i.e.* CO_2 / carbonate

or formic acid / formate). This proposition is based on the fact that glycerol can be fully oxidized to CO_2 on Pt, Pd and Au, together with the observation that glyceric acid and glycolic acid are the most commonly seen products beside DHA.[10–12,49,146] This proposed mechanism also matches the fact that oxalic acid, tartronic acid, and mesoxalic acid are not easily obtained unless a lower ratio of glycerol concentration to the concentration of OH^- is used,[2,36,46,112,147] which is likely to involve the electrooxidation of DHA, glyceric acid and glycolic acid. Furthermore, this model also supports the fact that glyoxylic acid, glycoaldehyde and formaldehyde are rarely found in most of the studies.

Looking at FTIR results obtained with Pt and Pd (spectra in Figure 5 and 6), CO(ads) and glyceraldehyde are generated in Stage I as a result of complete / partial deprotonation of a terminal carbon atom in the absence of OH(ads) (as in acidic solutions, or at very low overpotentials in alkaline solutions).[57,58,60] A trend towards carboxylic acid / carboxylate (mainly glyceric acid) is initiated when OH(ads) is generated (in Stage II), which strongly directs the reaction pathway towards carboxylate and therefore reduces the proportion of products from cleaved C-C bond.[74] (This reduction is enhanced by the alkalinity of the electrolyte.) As the overpotential progresses up, a rapid consumption of hydroxide (up to 20 times of the amount of glycerol molecules consumed) tends to re-direct the reaction pathway back to the acidic case.[130] Therefore, more C1/C2 products and CO_2 are generated in Stage III, which is synergized by the high overpotential applied to overcome the energy barrier of C-C cleavage (not yet confirmed because of the uncertain local pH). To sum up, a table (Table 2) lists the conditions for preferentially producing certain products from GEOR, and a diagram summarizing the reaction mechanism proposed in this paper is shown in Figure 11.

Table 2: Conditions for glycerol valorization with Pt, Pd and Au

No. of Carbon atoms	**Product**	**Produced directly / indirectly from glycerol?**	**Acidic / Alkaline**	**OH(ads) needed for direct production?**	**Remarks**
3	Glyceraldehyde	Directly	Acidic	No	low overpotentials and more (100) planes
3	Dihydroxyacetone	Directly	Acidic	No	(111) planes with Sb and Bi deposited
3	Glyceric Acid	Both (indirectly from glyceraldehyde)	Both	Yes	low overpotentials and strong alkaline electrolyte for massive production
3	Tartronic Acid	Indirectly from glyceric acid	Both	N/A	long term oxidation
3	Mesoxalic Acid	Indirectly from hydroxypyruvic acid	Unknown	N/A	
3	Hydroxypyruvic Acid	Both (indirectly from DHA, glyceric acid)	Both	Yes	(111) planes
3	Lactic Acid	Indirectly from glyceraldehyde	Acidic	N/A	deaerated
2	Glycolic Acid	Both (indirectly from glyceric acid)	Both	Yes	strong alkaline electrolyte for massive production
2	Oxalic Acid	Both (indirectly from glycolic acid)	Both	Yes	
2	Glyoxylic Acid	Unknown			
1	Formic Acid	Both (from glyceric acid, glycolic acid)	Both	Yes	strong alkaline electrolyte for massive production
1	CO_2 / Carbonate	Both (indirectly from glyceric acid, glycolic acid, formic acid)	Both	Yes	high overpotentials (>1.0 V vs RHE) for massive production

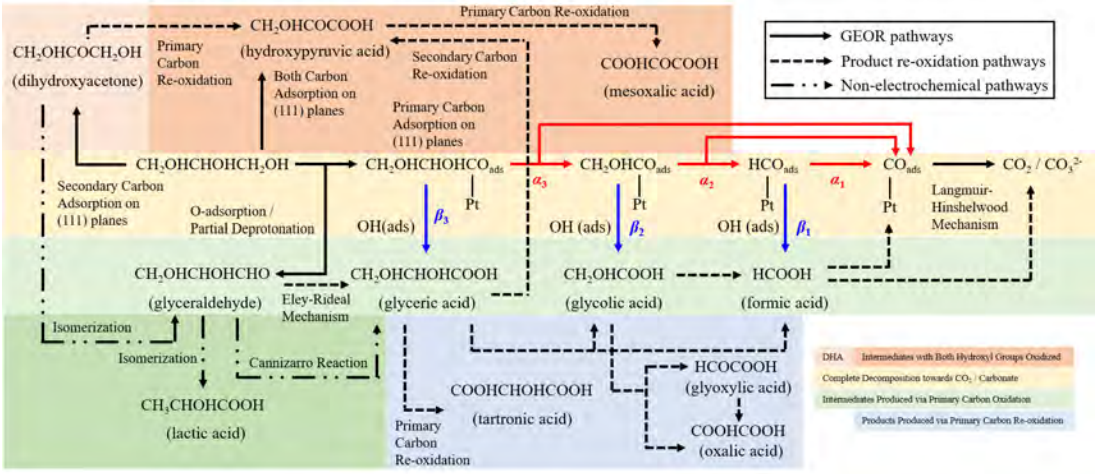

Figure 11: Proposed reaction mechanism of glycerol electrooxidation on Pt, Pd, and Au.

In this model, since the reaction of $R^{(n)}CO(ads)$ into the degraded $R^{(n-1)}CO(ads)$ is competing with other pathways towards carboxylates, α_n (C-C cleavage) and β_n (conversion into $R^{(n)}COOH$) are defined as the probabilities of these two processes, with the sum of α_n and β_n to be 1. The quantities α_n and β_n describe the preference of RCO(ads) towards each product, and therefore are a function of overpotential η, pH and the type of crystal plane ε, *i.e.*, α_n (η, pH, ε). The quantity β_n can be written as 1- α_n. Other factors possibly affecting α_n include but are not limited to temperature and pressure.

5 Electrocatalysts for Enhanced Efficiency and Selectivity of GEOR

There has been significant recent research on bi-/tri-/multi-metallic nanocatalysts and composites aimed at improving the efficiency of glycerol conversion and the selectivity towards certain products. This section summarizes the achievements and also controversies with respect to the performances of metallic catalysts reported so far. As Martins et al.[136] have commented, the properties of elec-

trocatalysts used for GEOR are subject to preparation processes which vary significantly between studies and between groups who conduct them. Also, conditions under which GEOR occurs lack uniformity, including even the choice of reference electrodes. It is barely possible to draw many conclusions under such circumstances, and future researchers are strongly urged to standardize their experimental conditions and give more mechanistic interpretations with tools like isotopic-labelling studies.

As illustrated in Figure 12, many nanocatalysts with novel structures have been synthesized.[7,85,148–154] Nanostructured catalysts (*e.g.* nano-dendrites,[91,155] nano-flowers) possess not only a higher specific surface area, but also the preferential growth on certain crystal planes. Also, they usually enjoy a large number of step and kink sites, as well as high-index planes that have a higher activity for catalysis. For example, Pd(520) has a higher catalytic activity compared with low-index planes. The reason is that it has a higher density of kinks (with dangling bonds) and steps which weaken the strength of C-C and C-H bonds.[11,85]

The catalytic performance of metallic electrocatalysts can be enhanced by alloying, introducing skin or shell overlayers, or introducing ad-atoms. In general, many studies have proven that adding other metals (*e.g.* oxophilic metals like Rh, Sn and Ni[156]) which have a lower onset potential of OH adsorption can efficiently prevent the CO poisoning effect on the modified metal surface.[109] Like metallic catalysts, metal oxides (*e.g.* NiO[157], CeO_2[158]), especially those with oxygen defects,[85] are also able to provide OH(ads) at a lower potential than the catalyst they modify.

Catalytic activities also depend on the electronic structures of the metallic substrates. With a downshifted d-band center, a metallic catalyst tends to adsorb more alcohol[39] (presumably the ability to cleave the C-H bond is improved) and form more M-OH(ads) which facilitates the oxidation of CO to CO_2. In this case, an overlap of the electronic orbitals of substrate metals (*e.g.* Pt (5d)) and transition metals (3d/4d) can occur,[159] which leads to a lowered d-band center and a destablized binding of intermediates. Researchers have revealed that amphoteric metals (*e.g.* Al and Ga) have similar effects as their 3p orbitals can mix with the Pt(5d) orbitals.[160] This downshift can also be induced by ad-atoms with a different work function, because they can induce electron transfer from substrate metals (*e.g.* Pt) to them, lowering of density of states near Fermi level of the substrate metals to reach an equilibrium between two metals,[2,161] and this electron transfer can prevent the oxidation of substrate metals.[40] In addition, the lattice strain generated by ad-atoms can also downshift the d-band center of the metal they modify, and the effectiveness of lattice strain depends on the difference between their lattice parameters.[162] This downshift would cause the back-donation of electrons from Pt (5d) to CO(ads) ($2p^*$), which reduces the bond strength of M-CO and promotes the CO removal.[2,142] It is also reported that the position of the d-band center (associated with the binding energy of intermediates) can be modulated by the morphology and shape of metallic nanoparticles.[163] The introduction of a second metal into the lattice may lead to the lattice distortion. In the case of PtFe nanocomposites,[136] a sublayer of Pt atoms is generated, which transfers electrons to the surface of Pt. As a result, the d-band electron density of surface Pt increases and promotes the cleavage of C-H bonds.

The ratio of metal A to metal B needs to be carefully determined since the introduced metal atoms may rearrange the locations and distribution of surface atoms. On one hand, the coverage of certain active sites[14] / crystal planes with a non-active metal (*e.g.* Ru preferentially deposited on Pt(111)[164]) can decrease the efficiency of oxidation. On the other hand, it is noteworthy that the product selectivity strongly depends on the type of metal introduced, as preferential deposition can restructure the surface atoms. For example, a study on the "ensemble effect" with different ratios of Ag to Pd yields Pd with different structures and properties with respect to adsorption.[26] Some atoms favor the defective sites with higher energy, whereas others prefer to deposit on a certain facet.[50] It is well known that three vicinal sites (*i.e.* atoms) on (111) facets are required to oxidize primary alcohols in the case of Pt and Pd. The reason is that the oxidation through primary

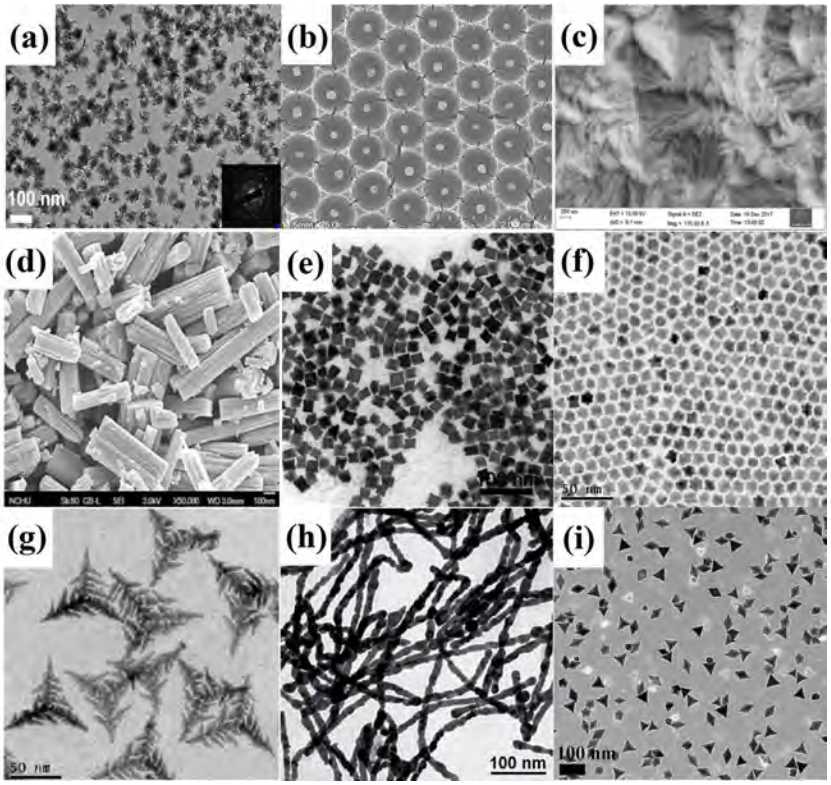

Figure 12: SEM pictures of various nanometallic electrocatalysts for GEOR. (a) Pd nanodendrites@rGO (Reprinted with permission from Ref[148], Copyright © 2013, Hydrogen Energy Publications, LLC. Published by Elsevier Ltd. All rights reserved.), (b) Au single nanoparticle@SiO_2 (Reprinted with permission from Ref[149], Copyright © 2014 Elsevier B.V. All rights reserved.), (c) Ni nanosponges (Reprinted with permission from Ref[7], © The Royal Society of Chemistry and the Centre National de la Recherche Scientifique 2019), (d) Pd@WO_x nanobundles (Reprinted with permission from Ref[85], Copyright © 2019 American Chemical Society), (e) PtSn nanocubes (Reprinted with permission from Ref[150], © 2018 Hydrogen Energy Publications LLC. Published by Elsevier Ltd. All rights reserved.), (f) PtCuCo hexagonal nanocrystals (Reprinted with permission from Ref[151], © 2018 Taiwan Institute of Chemical Engineers. Published by Elsevier B.V. All rights reserved.), (g) PtCu nano-tripods (Reprinted with permission from Ref[152], © The Royal Society of Chemistry 2018), (h) Pt nanowires (Reprinted with permission from Ref[153], © The Royal Society of Chemistry 2017), (i) Pd trigonal/pyramidal nanocrystals (Reprinted with permission from Ref[154], © 2017 Wiley-VCH Verlag GmbH &Co. KGaA, Weinheim).

carbon atom involves the cleavage of two C-H bonds and one O-H bond. Each bond dissociation requires an interaction with a surface atom.[50] Reducing the number of these ensembles lowers the efficiency of primary alcohol conversion, whereas secondary alcohol conversion is not affected as it only requires one Pt/Pd atom.[39] Benefitting from that, high selectivity towards DHA (partially converted to glyceraldehyde via isomerization[124] and further to glycerate if in strong alkali[121]) through the preferential oxidation of the secondary carbon can be achieved, as exemplified by Bi-modified,[54] Ru-modified,[146] and Sb-modified Pt.[14,53] Moreover, researchers have reported that Sb has a remarkably higher selectivity towards DHA (61.4%, obtained at 0.797 V vs RHE) than Bi (usually between 10-20%) and a higher potential of oxidation towards its oxide.[49]

Ag is a special ad-metal that can oxidize glycerol on its own (producing formate, glycolate and glycerate at 1.125 V vs RHE[165]). It can upshift the d-band center of the substrate metals (Pt, Pd and Au) to promote the adsorption between substrate metals and glycerol.[64,166] As a noble metal with similar lattice parameters to Au, it is found to promote the C-C bond cleavability of Pd and Au.[33,167,168] With the help of Ag, GEOR occurs on Au through C-C bond cleavage to produce formate and glycolate in alkaline media.[11] Ag-OH(ads) produced in strong alkaline media (pH > 11) has been shown to be the catalytic species, and not Ag[169] or Ag_2O (previously taken as a catalytic species,[92] but regarded as an inhibitor at present)[25].

The tailoring of GEOR with different ad-metals has been extensively studied. Rh shows little promotion on the catalytic efficiency[12] and C-C bond cleavage[170,171] when alloyed with Pt (still under debate[2,172]), whereas it facilitates the C-C bond cleavage on Pd.[130] Additionally, Rh shows reactivity through primary carbon oxidation and C-C bond dissociation on its own.[173] Ru can provide OH(ads) at lower potentials to promote GEOR,[12] facilitate the dissociation of C-C bonds on Pd, and increase the selectivity towards glycerate (with Pd) or DHA (with Pt) in alkaline condition,[146,174] while it has no capability of oxidizing glycerol by itself.[175] Other reported observations include the production of DHA and glycolic acid with a Pt-Ru electrocatalyst, and the weakened binding energy of glycerol onto the PtRu surface in acidic solutions.[132]

Other commonly investigated ad-metals include Sb, Bi, Pb, In and Sn. Sb and Bi tend to oxidize the secondary hydroxyl groups (via chelating and blocking effects as shown in Figure 13, as Bi chelates with secondary alcohol groups), while Pb and In promote the primary alcohol oxidation.[53] Sb is believed to facilitate C-C bond breakage at Pt under alkaline condition,[124] while others discovered an inhibiting effect in an acidic solution.[158] Whether Sn can promote the dissociation of C-C bonds with Pt catalysts is still under debate.[176,177]

The conversion to CO_2 from glycerol with Ni electrodes can be increased by involving elements from the same group (*e.g.* Co and Fe). The enhancement can be attributed to CoOOH converted from $Co(OH)_2$, which occurs at a lower overpotential compared with the conversion of $Ni(OH)_2$ to NiOOH.[121]

To make multi-metallic catalysts, electrodeposition is a method commonly adopted. The epitaxial relationship of the deposit to the substrate is strongly influenced by the potential used for electrodeposition. It is also believed that the attachment of metallic catalysts onto carbon supports can change the electronic structure of metals, and consequently change the bonding strength with adsorbates. This modified electronic structure improves the adsorption of glycerol onto metals.[178] In addition, the interaction between metallic catalysts (*e.g.* nanoparticles) and carbon supports can leave defects on the metal surfaces, which are highly active sites for catalysis.[179] The defects on a carbon support are deemed as high-energy sites which could facilitate nucleation of metallic nanostructures and their further growth.[2] Taking single-wall carbon nanotube (SWNT) as an example, the preferential decoration of defect sites rather than sp^2-bonded lattice sites can be achieved by modulating the electrodeposition potentials.[180]

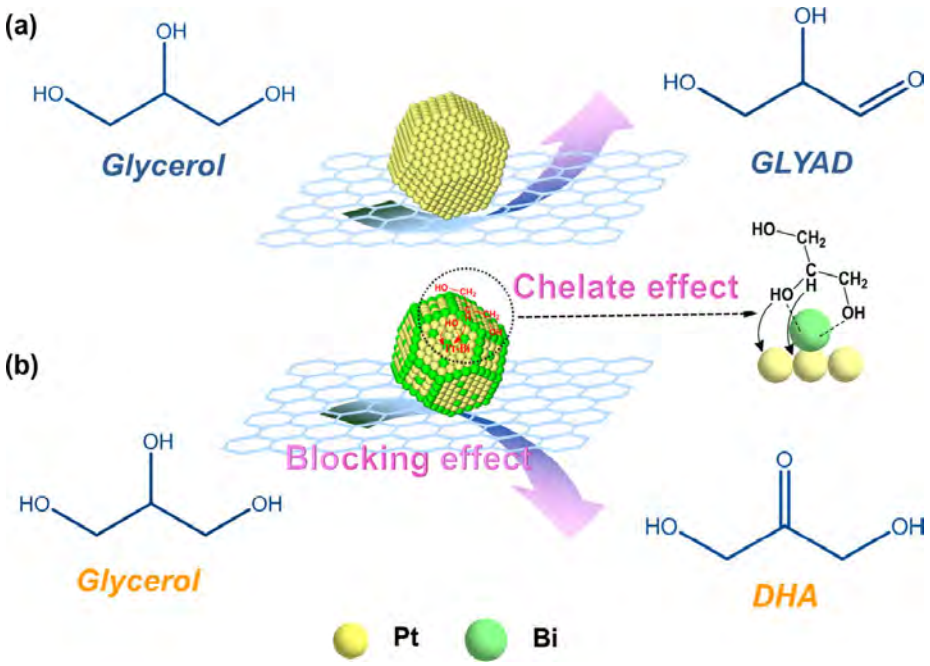

Figure 13: Scheme showing the blocking and chelate effects of Bi adatoms to Pt/NCNT electrocatalyst. (Reprinted with permission from Ref[14], © 2016 Elsevier Inc. All rights reserved.).

6 Summary and Outlook

Glycerol electrooxidation has been shown to be a very promising way of generating value-added products. High selectivity towards certain products has been reported, including but not limited to DHA, glyceric acid and glycolic acid. However, the investigation of mechanism of glycerol valorization is still an open area of research. One of the key reasons is that the complete oxidation of glycerol into CO_2 consumes 20 OH^- ions per molecule (together with 14 electrons transferred), causing a significant change in the pH at the electrode, which may re-direct the reaction to other products and eventually affect the interpretation of reaction mechanisms.[181] Moreover, uncertainty is introduced by the diversity of catalysts used for GEOR. Unlike most studies arguing that C1/C2 products are generated from the oxidation of C2/C3 products, this review provides a prospective in which all side products are generated directly from glycerol via $CH_2OHCHOHCO$(ads), CH_2OHCO(ads), and HCO(ads), supported by the observations that no side products have shown a higher electrochemical reactivity than glycerol. Based on the GEOR model proposed in this review, statements regarding C-C bond cleavability should be re-assessed because the cleavabilities of two C-C bonds are obviously different under the same conditions. Also, the proposition that Pd has a weaker ability to cleave C-C bonds than Pt has been clarified: this weaker ability is due to the lack of deprotonation efficiency without Pd-OH(ads). As Martins et al.[18] commented, more studies on multi-metallic catalysts should be carried out, with detailed reporting and standard conditions of catalyst preparations to better reveal the real reaction mechanisms. However, as many differences exist in the experimental conditions which cannot be easily unified, great efforts should be made by future researchers into fundamental studies of GEOR using advanced surface characterization methods and isotopic-labelling studies.

Examples of other interesting observations which are worthy to be further investigated include:

- Coutanceau et al.[137] reported that hydroxypyruvate and C2/C1 products were produced simultaneously with Pd-Sn nanoparticles, as hydroxypyruvate is a rarely found product.
- The conversion of glyceric acid to lactic acid as a byproduct of GEOR is a special case, as it is either not found in the mixture of products (mostly reported) or found to be a large amount.[36]
- Ni has been found as an effective catalyst for GEOR which has the potential of replacing noble metals. The oxidation of alcohol to aldehyde and furthur to carboxylate has been widely recognized. Also, the cleavage of C-C bonds of glycerol with β-NiOOH to produce formate and carbonate are commonly observed. Throwing lights on this issue is a promising research hotspot.

Acknowledgement 1 *This work was financially supported by the Natural Sciences and Engineering Research Council of Canada through its Discovery Frontiers program (Engineered Nickel Catalysts for Electrochemical Clean Energy project ("Ni Electro Can") administered from Queen's University), Discovery Grants program and CREATE program (Materials for Enhanced Energy Technologies ("MEET") project), and by the Research Council of Norway through its International Partnerships Program (Canada-Norway Partnership in Electrochemical Energy Technologies ("CANOPENER") project). The financial support from the above-mentioned funding agencies is highly appreciated.*

Table of Contents Graphic

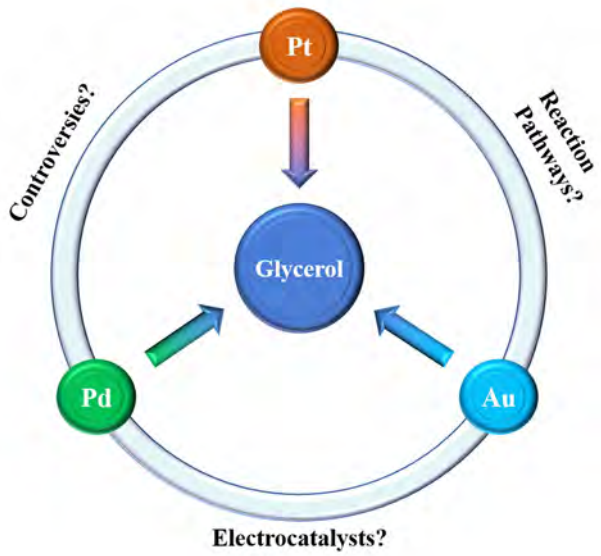

The valorization of glycerol through its electrooxidation has been widely conducted with Pt, Pd, and Au electrodes. However, the controversies brought by reported experimental results prevent us from understanding the reaction mechanisms. This review summarized key observations of glycerol electrooxidation at these electrodes, and proposed new reaction pathways.

Keywords

Glycerol oxidation, Platinum, Palladium, Gold, Carboxylic acids.

References

[1] S. D. Minteer, *Int. Mater. Rev.* **2018**, *63*, 241–256.

[2] Y. Zhou, Y. Shen, J. Piao, *ChemElectroChem* **2018**, *5*, 1636–1643.

[3] L. Du, Y. Shao, J. Sun, G. Yin, C. Du, Y. Wang, *Catal. Sci. and Technol.* **2018**, *8*, 3216–3232.

[4] P. Song, H. Xu, J. Wang, Y. Zhang, F. Gao, F. Ren, Y. Shiraishi, C. Wang, Y. Du, *J. Taiwan Inst. Chem. Eng.* **2018**, *93*, 616–624.

[5] T. Nitaya, Y. Cheng, S. Lu, K. Poochinda, K. Pruksathorn, S. P. Jiang, *Chem. Commun.* **2018**, *54*, 12404–12407.

[6] Y. Wang, T. Kou, H. Gao, J. Niu, J. Zhang, L. Lv, Z. Peng, Z. Zhang, *J. Mater. Chem.A* **2018**, *6*, 10525–10534.

[7] P. Sivasakthi, M. V. Sangaranarayanan, *New J. Chem.* **2019**, *43*, 8352–8362.

[8] G. Y. Hou, Y. Y. Xie, L. K. Wu, H. Z. Cao, Y. P. Tang, G. Q. Zheng, *Int. J. Hydrogen Energy* **2016**, *41*, 9295–9302.

[9] V. L. Oliveira, C. Morais, K. Servat, T. W. Napporn, P. Olivi, K. B. Kokoh, G. Tremiliosi-Filho, *Electrocatalysis* **2015**, *6*, 447–454.

[10] J. Han, Y. Kim, D. H. K. Jackson, K. E. Jeong, H. J. Chae, K. Y. Lee, H. J. Kim, *Electrochem. Commun.* **2018**, *96*, 16–21.

[11] L. Thia, M. Xie, D. Kim, X. Wang, *Catal. Sci. Technol.* **2017**, *7*, 874–881.

[12] L. Huang, J. Y. Sun, S. H. Cao, M. Zhan, Z. R. Ni, H. J. Sun, Z. Chen, Z. Y. Zhou, E. G. Sorte, Y. Y. J. Tong, S. G. Sun, *ACS Catal.* **2016**, *6*, 7686–7695.

[13] E. Ferreira Frota, V. V. Silva de Barros, B. R. S. de Araújo, Â. Gonzaga Purgatto, J. J. Linares, *Int. J. Hydrogen Energy* **2017**, *42*, 23095–23106.

[14] X. Ning, Y. Li, H. Yu, F. Peng, H. Wang, Y. Yang, *J. Catal.* **2016**, *335*, 95–104.

[15] B. Wang, L. Tao, Y. Cheng, F. Yang, Y. Jin, C. Zhou, H. Yu, Y. Yang, *Catalysts* **2019**, *9*, 387.

[16] Y. Liu, W. Yu, D. Raciti, D. H. Gracias, C. Wang, *J. Phys. Chem. C* **2019**, *123*, 426–432.

[17] A. A. Nascimento, L. M. Alencar, C. R. Zanata, E. Teixeira-Neto, A. P. Mangini, G. A. Camara, M. A. Trindade, C. A. Martins, *Electrocatalysis* **2019**, *10*, 82–94.

[18] M. Trindade, *Increased Biodiesel Efficiency*, **2018**.

[19] C. S. Lee, M. K. Aroua, W. A. Wan Daud, P. Cognet, Y. Pérès, M. A. Ajeel, *Front. Chem.* **2019**, *7*, 1–11.

[20] C. Coutanceau, S. Baranton, *Wiley Interdiscip. Rev.: Energy Environ.* **2016**, *5*, 388–400.

[21] M. Simões, S. Baranton, C. Coutanceau, *ChemSusChem* **2012**, *5*, 2106–2124.

[22] J. F. Gomes, V. L. Oliveira, P. M. Pratta, G. Tremiliosi-Filho, *Electrocatalysis* **2014**, *6*, 7–19.

[23] C. Coutanceau, S. Baranton, R. S. Kouamé, *Front. Chem.* **2019**, *7*, 1–15.

[24] M. S. Houache, K. Hughes, E. A. Baranova, *Sustainable Energy Fuels* **2019**, *3*, 1892–1915.

[25] C. A. Angelucci, J. Souza-Garcia, P. S. Fernández, P. V. Santiago, R. M. Sandrini, *Encycl. of Interfacial Chem.: Surface Sci. and Electrochem.* **2018**, 643–650.

[26] N. Cai, C. Jin, C. Wan, R. Dong, *J. Electrochem. Soc.* **2017**, *164*, H437—-H442.

[27] O. Enea, J. P. Ango, *Electrochim. Acta* **1989**, *34*, 391–397.

[28] A. Hilmi, E. M. Belgsir, J. M. Le ÌĄger, C. Lamy, *J. Electroanal. Chem.* **1995**, *380*, 177–184.

[29] M. Simões, S. Baranton, C. Coutanceau, *Appl. Catal., B* **2010**, *93*, 354–362.

[30] Y. Kwon, K. J. P. Schouten, M. T. Koper, *ChemCatChem* **2011**, *3*, 1176–1185.

[31] J. R. McManus, E. Martono, J. M. Vohs, *Catal. Today* **2014**, *237*, 157–165.

[32] I. Takigawa, K. I. Shimizu, K. Tsuda, S. Takakusagi, *RSC Adv.* **2016**, *6*, 52587–52595.

[33] A. C. Garcia, M. J. Kolb, C. Van Nierop Y Sanchez, J. Vos, Y. Y. Birdja, Y. Kwon, G. Tremiliosi-Filho, M. T. Koper, *ACS Catal.* **2016**, *6*, 4491–4500.

[34] Y. Kwon, S. C. Lai, P. Rodriguez, M. T. Koper, *J. Am. Chem. Soc.* **2011**, *133*, 6914–6917.

[35] Y. Y. Birdja, M. T. Koper, *J. Am. Chem. Soc.* **2017**, *139*, 2030–2034.

[36] C. Dai, L. Sun, H. Liao, B. Khezri, R. D. Webster, A. C. Fisher, Z. J. Xu, *J. Catal.* **2017**, *356*, 14–21.

[37] C. C. Lima, M. V. Rodrigues, A. F. Neto, C. R. Zanata, C. T. Pires, L. S. Costa, J. Solla-Gullón, P. S. Fernández, *Appl. Catal., B* **2020**, *279*, 119369.

[38] M. B. De Souza, V. Y. Yukuhiro, R. A. Vicente, C. T. Vilela Menegaz Teixeira Pires, J. L. Bott-Neto, P. S. Fernández, *ACS Catal.* **2020**, *10*, 2131–2137.

[39] R. M. Castagna, J. M. Sieben, A. E. Alvarez, M. M. E. Duarte, *Int. J. Hydrogen Energy* **2019**, *44*, 5970–5982.

[40] Y. Zhou, Y. Shen, J. Xi, *Appl. Catal., B* **2019**, *245*, 604–612.

[41] B. Liu, J. Greeley, *J. Phys. Chem. C* **2011**, *115*, 19702–19709.

[42] G. Soffiati, J. L. Bott-Neto, V. Y. Yukuhiro, C. T. Pires, C. C. Lima, C. R. Zanata, Y. Y. Birdja, M. T. Koper, M. A. San-Miguel, P. S. Fernández, *J. Phys. Chem. C* **2020**, *124*, 14745–14751.

[43] J. Schnaidt, M. Heinen, Z. Jusys, R. J. Behm, *Electrochim. Acta* **2013**, *104*, 505–517.

[44] L. Roquet, E. M. Belgsir, J. M. Léger, C. Lamy, *Electrochim. Acta* **1994**, *39*, 2387–2394.

[45] P. Saila, M. Hunsom, *Korean J. Chem. Eng.* **2015**, *32*, 2412–2417.

[46] L. S. Ribeiro, E. G. Rodrigues, J. J. Delgado, X. Chen, M. F. R. Pereira, J. J. M. Órfão, *Ind. Eng. Chem. Res.* **2016**, *55*, 8548–8556.

[47] F. Frusteri, F. Arena, G. Bonura, C. Cannilla, L. Spadaro, O. Di Blasi, *Appl. Catal., A* **2009**, *367*, 77–83.

[48] J. González-Cobos, S. Baranton, C. Coutanceau, *J. Phys. Chem. C* **2016**, *120*, 7155–7164.

[49] S. Lee, H. J. Kim, E. J. Lim, Y. Kim, Y. Noh, G. W. Huber, W. B. Kim, *Green Chem.* **2016**, *18*, 2877–2887.

[50] A. Zalineeva, S. Baranton, C. Coutanceau, *Electrochim. Acta* **2015**, *176*, 705–717.

[51] M. Hunsom, P. Saila, *Int. J. Electrochem. Sci.* **2013**, *8*, 11288–11300.

[52] A. Zalineeva, S. Baranton, C. Coutanceau, *Electrochem. Commun.* **2013**, *34*, 335–338.

[53] Y. Kwon, T. J. P. Hersbach, M. T. M. Koper, *Top. Catal.* **2014**, *57*, 1272–1276.

[54] Y. Kwon, Y. Birdja, I. Spanos, P. Rodriguez, M. T. Koper, *ACS Catal.* **2012**, *2*, 759–764.

[55] M. Simões, S. Baranton, C. Coutanceau, *Appl. Catal., B* **2011**, *110*, 40–49.

[56] J. F. Gomes, G. Tremiliosi-Filho, *Electrocatalysis* **2011**, *2*, 96–105.

[57] P. S. Fernández, M. E. Martins, G. A. Camara, *Electrochim. Acta* **2012**, *66*, 180–187.

[58] C. A. Martins, M. J. Giz, G. A. Camara, *Electrochim. Acta* **2011**, *56*, 4549–4553.

[59] P. S. Fernández, P. Tereshchuk, C. A. Angelucci, J. F. Gomes, A. C. Garcia, C. A. Martins, G. A. Camara, M. E. Martins, J. L. F. Da Silva, G. Tremiliosi-Filho, *Phys. Chem. Chem. Phys.* **2016**, *18*, 25582–25591.

[60] J. Schnaidt, M. Heinen, D. Denot, Z. Jusys, R. Jürgen Behm, *J. Electroanal. Chem.* **2011**, *661*, 250–264.

[61] J. F. Gomes, F. B. C. De Paula, L. H. S. Gasparotto, G. Tremiliosi-Filho, *Electrochim. Acta* **2012**, *76*, 88–93.

[62] R. M. L. M. Sandrini, J. R. Sempionatto, E. Herrero, J. M. Feliu, J. Souza-Garcia, C. A. Angelucci, *Electrochem. Commun.* **2018**, *86*, 149–152.

[63] P. S. Fernández, C. A. Martins, C. A. Angelucci, J. F. Gomes, G. A. Camara, M. E. Martins, G. Tremiliosi-Filho, *ChemElectroChem* **2015**, *2*, 263–268.

[64] Y. Holade, C. Morais, K. Servat, T. W. Napporn, K. B. Kokoh, *ACS Catal.* **2013**, *3*, 2403–2411.

[65] A. Kabbabi, R. Faure, R. Durand, B. Beden, F. Hahn, J. M. Leger, C. Lamy, *J. Electroanal. Chem.* **1998**, *444*, 41–53.

[66] S. Zou, R. Gómez, M. J. Weaver, *J. Electroanal. Chem.* **1999**, *474*, 155–166.

[67] S. Zou, R. Gómez, M. J. Weaver, *Surf. Sci.* **1998**, *399*, 270–283.

[68] K. I. Ozoemena, *RSC Adv.* **2016**, *6*, 89523–89550.

[69] O. Muneeb, J. Estrada, L. Tran, K. Nguyen, J. Flores, S. Hu, A. M. Fry-Petit, L. Scudiero, S. Ha, J. L. Haan, *Electrochim. Acta* **2016**, *218*, 133–139.

[70] E. Habibi, H. Razmi, *Int. J. Hydrogen Energy* **2012**, *37*, 16800–16809.

[71] L. Su, W. Jia, A. Schempf, Y. Lei, *Electrochem. Commun.* **2009**, *11*, 2199–2202.

[72] A. Kahyaoglu, B. Beden, C. Lamy, *Electrochim. Acta* **1984**, *29*, 1489–1492.

[73] A. Zalineeva, A. Serov, M. Padilla, U. Martinez, K. Artyushkova, S. Baranton, C. Coutanceau, P. Atanassov, *Electrochem. Commun.* **2015**, *57*, 48–51.

[74] A. Zalineeva, A. Serov, M. Padilla, U. Martinez, K. Artyushkova, S. Baranton, C. Coutanceau, P. B. Atanassov, *J. Am. Chem. Soc.* **2014**, *136*, 3937–3945.

[75] C. Bianchini, P. K. Shen, *Chem. Rev.* **2009**, *109*, 4183–4206.

[76] T. Hu, Y. Wang, Q. Liu, L. Zhang, H. Wang, T. Tang, W. Chen, M. Zhao, J. Jia, *Int. J. Hydrogen Energy* **2017**, *42*, 25951–25959.

[77] G. A. B. Mello, C. Busó-Rogero, E. Herrero, J. M. Feliu, *J. Chem. Phys.* **2019**, *150*.

[78] H. A. Miller, M. Bellini, F. Vizza, C. Hasenöhrl, R. D. Tilley, *Catal. Sci. Technol.* **2016**, *6*, 6870–6878.

[79] A. C. Garcia, Y. Y. Birdja, G. Tremiliosi-Filho, M. T. Koper, *J. Catal.* **2017**, *346*, 117–124.

[80] S. Feng, J. Yi, H. Miura, H. Miura, H. Miura, N. Nakatani, M. Hada, T. Shishido, T. Shishido, T. Shishido, T. Shishido, *ACS Catal.* **2020**, *10*, 6071–6083.

[81] C. Jin, X. Sun, Z. Chen, *Chem. Eng. Technol.* **2012**, *35*, 1064–1068.

[82] W. Hong, P. Bi, C. Shang, J. Wang, E. Wang, *J. Mater. Chem.A* **2016**, *4*, 4485–4489.

[83] Y. Zhou, Y. Shen, *Electrochem. Commun.* **2018**, *90*, 106–110.

[84] K. E. Guima, L. M. Alencar, G. C. Da Silva, M. A. G. Trindade, C. A. Martins, *ACS Sustainable Chem. Eng.* **2018**, *6*, 1202–1207.

[85] L. Karuppasamy, C. Y. Chen, S. Anandan, J. J. Wu, *ACS Appl. Mater. Interfaces* **2019**, *11*, 10028–10041.

[86] B. N. Zope, D. D. Hibbitts, M. Neurock, R. J. Davis, *Science* **2010**, *330*, 74–78.

[87] X. Shi, D. E. Simpson, D. Roy, *Phys. Chem. Chem. Phys.* **2015**, *17*, 11432–11444.

[88] Y. Chen, L. Zhuang, J. Lu, *Chin. J. Catal.* **2007**, *28*, 870–874.

[89] C. A. Ottoni, S. G. da Silva, R. F. B. De Souza, A. O. Neto, *Ionics* **2016**, *22*, 1167–1175.

[90] Z. Zhang, L. Xin, W. Li, *Int. J. Hydrogen Energy* **2012**, *37*, 9393–9401.

[91] J. L. Bott-Neto, A. C. Garcia, V. L. Oliveira, N. E. De Souza, G. Tremiliosi-Filho, *J. Electroanal. Chem.* **2014**, *735*, 57–62.

[92] M. Avramov-Ivić, V. Jovanović, G. Vlajnić, J. Popić, *J. Electroanal. Chem.* **1997**, *423*, 119–124.

[93] C. A. Angelucci, H. Varela, G. Tremiliosi-Filho, J. F. Gomes, *Electrochem. Commun.* **2013**, *33*, 10–13.

[94] S. C. Lai, S. E. Kleijn, F. T. Öztürk, V. C. Van Rees Vellinga, J. Koning, P. Rodriguez, M. T. Koper, *Catal. Today* **2010**, *154*, 92–104.

[95] X. Cui, Y. Li, M. Zhao, Y. Xu, L. Chen, S. Yang, Y. Wang, *Nano Res.* **2019**, *12*, 351–356.

[96] M. Mougenot, A. Caillard, M. Simoes, S. Baranton, C. Coutanceau, P. Brault, *Appl. Catal., B* **2011**, *107*, 372–379.

[97] J. Monzó, Y. Malewski, F. J. Vidal-Iglesias, J. Solla-Gullon, P. Rodriguez, *ChemElectroChem* **2015**, *2*, 958–962.

[98] D. L. Zhou, R. Z. Wang, M. Zhang, X. Weng, J. R. Chen, A. J. Wang, J. J. Feng, *Electrochim. Acta* **2013**, *108*, 390–397.

[99] R. R. Adžić, M. Avramov-Ivić, *J. Catal.* **1986**, *101*, 532–535.

[100] I. T. Schwartz, A. P. Jonke, M. Josowicz, J. Janata, *Catal. Lett.* **2013**, *143*, 777–782.

[101] P. Ocón, C. Alonso, R. Celdrán, J. González-Velasco, *J. Electroanal. Chem.* **1986**, *206*, 179–196.

[102] K. N. Heck, B. G. Janesko, G. E. Scuseria, N. J. Halas, M. S. Wong, *ACS Catal.* **2013**, *3*, 2430–2435.

[103] N. Yahya, S. K. Kamarudin, N. A. Karim, M. S. Masdar, K. S. Loh, K. L. Lim, *Energy Convers. Manage.* **2019**, *188*, 120–130.

[104] P. Rodriguez, N. Garcia-Araez, M. T. Koper, *Phys. Chem. Chem. Phys.* **2010**, *12*, 9373–9380.

[105] P. Rodríguez, A. A. Koverga, M. T. Koper, *Angew. Chem. Int. Ed.* **2010**, *49*, 1241–1243.

[106] P. Rodriguez, Y. Kwon, M. T. Koper, *Nat. Chem.* **2012**, *4*, 177–182.

[107] Y. Zhang, X. Zhu, J. Guo, X. Huang, *ACS Appl. Mater. Interfaces* **2016**, *8*, 20642–20649.

[108] C. A. Angelucci, R. C. Ambrosio, A. A. Gewirth, *ACS Catal.* **2018**, *8*, 2247–2252.

[109] N. Benipal, J. Qi, Q. Liu, W. Li, *Appl. Catal., B* **2017**, *210*, 121–130.

[110] C. A. Ottoni, S. G. da Silva, R. F. B. De Souza, A. O. Neto, *Electrocatalysis* **2016**, *7*, 22–32.

[111] S. Yongprapat, A. Therdthianwong, S. Therdthianwong, *J. Appl. Electrochem.* **2012**, *42*, 483–490.

[112] J. Qi, L. Xin, D. J. Chadderdon, Y. Qiu, Y. Jiang, N. Benipal, C. Liang, W. Li, *Appl. Catal., B* **2014**, *154-155*, 360–368.

[113] Z. Zhang, L. Xin, J. Qi, D. J. Chadderdon, K. Sun, K. M. Warsko, W. Li, *Appl. Catal., B* **2014**, *147*, 871–878.

[114] Z. Zhang, L. Xin, J. Qi, Z. Wang, W. Li, *Green Chem.* **2012**, *14*, 2150–2152.

[115] M. Valter, M. Busch, B. Wickman, H. Grönbeck, J. Baltrusaitis, A. Hellman, *J. Phys. Chem. C* **2018**, *122*, 10489–10494.

[116] E. G. Rodrigues, M. F. Pereira, X. Chen, J. J. Delgado, J. J. Órfão, *Ind. Eng. Chem. Res.* **2013**, *52*, 17390–17398.

[117] G. Vértes, G. Horányi, *J. Electroanal. Chem.* **1974**, *52*, 47–53.

[118] A. A. El-Shafei, *J. Electroanal. Chem.* **1999**, *471*, 89–95.

[119] J. H. Sinfelt, *Adv. Catal.* **1973**, *23*, 91–119.

[120] X. Liang, M. Xiao, M. Xu, D. Yang, Y. Yan, Y. Tian, Y. Miao, *J. Appl. Electrochem.* **2016**, *46*, 1–8.

[121] V. L. Oliveira, C. Morais, K. Servat, T. W. Napporn, G. Tremiliosi-Filho, K. B. Kokoh, *J. Electroanal. Chem.* **2013**, *703*, 56–62.

[122] V. L. Oliveira, C. Morais, K. Servat, T. W. Napporn, G. Tremiliosi-Filho, K. B. Kokoh, *Electrochim. Acta* **2014**, *117*, 255–262.

[123] T. Iwasita, F. C. Nart, *Prog. Surf. Sci.* **1997**, *55*, 271–340.

[124] T. P. Scachetti, A. C. D. Angelo, *Electrocatalysis* **2015**, *6*, 472–480.

[125] C. A. Martins, P. S. Fernández, H. E. Troiani, M. E. Martins, G. A. Camara, *J. Electroanal. Chem.* **2014**, *717-718*, 231–236.

[126] Y. Holade, C. Morais, S. Arrii-Clacens, K. Servat, T. W. Napporn, K. B. Kokoh, *Electrocatalysis* **2013**, *4*, 167–178.

[127] S. Rangarajan, R. R. Brydon, A. Bhan, P. Daoutidis, *Green Chem.* **2014**, *16*, 813–823.

[128] B. Liu, J. Greeley, *Phys. Chem. Chem. Phys.* **2013**, *15*, 6475–6485.

[129] B. T. X. Lam, M. Chiku, E. Higuchi, H. Inoue, *J. Power Sources* **2015**, *297*, 149–157.

[130] R. S. Ferreira, M. Janete Giz, G. A. Camara, *J. Electroanal. Chem.* **2013**, *697*, 15–20.

[131] T. S. D. Almeida, K. E. Guima, R. M. Silveira, G. C. Da Silva, M. A. U. Martines, C. A. Martins, *RSC Adv.* **2017**, *7*, 12006–12016.

[132] Y. Kim, H. W. Kim, S. Lee, J. Han, D. Lee, J. R. Kim, T. W. Kim, C. U. Kim, S. Y. Jeong, H. J. Chae, B. S. Kim, H. Chang, W. B. Kim, S. M. Choi, H. J. Kim, *ChemCatChem* **2017**, *9*, 1683–1690.

[133] L. M. Palma, T. S. Almeida, V. L. Oliveira, G. Tremiliosi-Filho, E. R. Gonzalez, A. R. De Andrade, K. Servat, C. Morais, T. W. Napporn, K. B. Kokoh, *RSC Adv.* **2014**, *4*, 64476–64483.

[134] M. B. De Souza, R. A. Vicente, V. Y. Yukuhiro, C. T. Pires, W. Cheuquepán, J. L. Bott-Neto, J. Solla-Gullón, P. S. Fernández, *ACS Catal.* **2019**, *9*, 5104–5110.

[135] S. Dash, N. Munichandraiah, *J. Electrochem. Soc.* **2013**, *160*, 197–202.

[136] X. Jin, H. Yan, C. Zeng, P. S. Thapa, B. Subramaniam, R. V. Chaudhari, *Ind. Eng. Chem. Res.* **2017**, *56*, 13157–13164.

[137] A. Zalineeva, A. Serov, M. Padilla, U. Martinez, K. Artyushkova, S. Baranton, C. Coutanceau, P. B. Atanassov, *Appl. Catal., B* **2015**, *176-177*, 429–435.

[138] L. M. Alencar, C. A. Martins, *Electroanalysis* **2018**, *30*, 2167–2175.

[139] T. Asset, A. Serov, M. Padilla, A. J. Roy, I. Matanovic, M. Chatenet, F. Maillard, P. Atanassov, *Electrocatalysis* **2018**, *9*, 480–485.

[140] A. Serov, T. Asset, M. Padilla, I. Matanovic, U. Martinez, A. Roy, K. Artyushkova, M. Chatenet, F. Maillard, D. Bayer, C. Cremers, P. Atanassov, *Appl. Catal., B* **2016**, *191*, 76–85.

[141] J. Han, Y. Kim, H. W. Kim, D. H. K. Jackson, D. Lee, H. Chang, H. J. Chae, K. Y. Lee, H. J. Kim, *Electrochem. Commun.* **2017**, *83*, 46–50.

[142] N. Yahya, S. K. Kamarudin, N. A. Karim, S. Basri, A. M. Zanoodin, *Nanoscale Res. Lett.* **2019**, *14*.

[143] G. B. Melle, E. G. Machado, L. H. Mascaro, E. Sitta, *Electrochim. Acta* **2019**, *296*, 972–979.

[144] Z. Zhang, L. Xin, J. Qi, D. J. Chadderdon, W. Li, *Appl. Catal., B* **2013**, *136-137*, 29–39.

[145] T. Pabisiak, M. J. Winiarski, A. Kiejna, *J. Chem. Phys.* **2016**, *144*, 044704.

[146] L. M. Palma, T. S. Almeida, C. Morais, T. W. Napporn, K. B. Kokoh, A. R. de Andrade, *ChemElectroChem* **2017**, *4*, 39–45.

[147] Z. Chen, C. Liu, X. Zhao, H. Yan, J. Li, P. Lyu, Y. Du, S. Xi, K. Chi, X. Chi, H. Xu, X. Li, W. Fu, K. Leng, S. J. Pennycook, S. Wang, K. P. Loh, *Adv. Mater.* **2019**, *31*, 1–8.

[148] S. S. Li, Y. Y. Hu, J. J. Feng, Z. Y. Lv, J. R. Chen, A. J. Wang, *Int. J. Hydrogen Energy* **2014**, *39*, 3730–3738.

[149] N. Li, Q. Zhou, X. Li, W. Chu, J. Adkins, J. Zheng, *Sens. Actuators, B* **2014**, *196*, 314–320.

[150] Z. Li, G. Qiu, Z. Jiang, W. Zhuang, J. Wu, X. Du, *Int. J. Hydrogen Energy* **2018**, *43*, 22538–22547.

[151] C. Zhai, J. Hu, H. Gao, L. Zeng, M. Xue, Z. Q. Liu, M. Zhu, *J. Taiwan Inst. Chem. Eng.* **2018**, *93*, 477–484.

[152] H. Xu, P. Song, F. Gao, Y. Shiraishi, Y. Du, *Nanoscale* **2018**, *10*, 8246–8252.

[153] N. Zhang, Y. Zhu, Q. Shao, X. Zhu, X. Huang, *J. Mater. Chem.A* **2017**, *5*, 18977–18983.

[154] C. Shang, W. Hong, Y. Guo, J. Wang, E. Wang, *Chem. - Eur. J.* **2017**, *23*, 5799–5803.

[155] Y. Zuo, L. Wu, K. Cai, T. Li, W. Yin, D. Li, N. Li, J. Liu, H. Han, *ACS Appl. Mater. Interfaces* **2015**, *7*, 17725–17730.

[156] H. Lv, L. Sun, D. Xu, S. L. Suib, B. Liu, *Green Chem.* **2019**, *21*, 2367–2374.

[157] M. C. Moraes, G. G. Junco, T. F. M. Moreira, C. J. G. Pinheiro, P. Olivi, D. Profeti, L. P. R. Profeti, *J. Environ. Chem. Eng.* **2019**, *7*, 102922.

[158] Q. He, Y. Shen, K. Xiao, J. Xi, X. Qiu, *Int. J. Hydrogen Energy* **2016**, *41*, 20709–20719.

[159] X. Y. Lang, G. F. Han, B. B. Xiao, L. Gu, Z. Z. Yang, Z. Wen, Y. F. Zhu, M. Zhao, J. C. Li, Q. Jiang, *Adv. Funct. Mater.* **2015**, *25*, 230–237.

[160] Y. Wang, Z. Wang, J. Zhang, C. Zhang, H. Gao, J. Niu, Z. Zhang, *Nanoscale* **2018**, *10*, 17070–17079.

[161] O. Muneeb, J. Estrada, T. Tran, S. Hu, B. Khorasani, A. Fry-Petit, L. Scudiero, S. Ha, J. L. Haan, *ChemistrySelect* **2017**, *2*, 9261–9266.

[162] C. Jin, J. Zhang, R. Dong, Q. Huo, *Int. J. Electrochem. Sci.* **2014**, *9*, 5743–5750.

[163] C. Wang, P. Song, F. Gao, T. Song, Y. Zhang, C. Chen, L. Li, L. Jin, Y. Du, *J. Colloid Interface Sci.* **2019**, *544*, 284–292.

[164] B. Tam, M. Duca, A. Wang, M. Fan, S. Garbarino, D. Guay, *ChemElectroChem* **2019**, 1784–1793.

[165] N. Y. Suzuki, P. V. B. Santiago, T. S. Galhardo, W. A. Carvalho, J. Souza-Garcia, C. A. Angelucci, *J. Electroanal. Chem.* **2016**, *780*, 391–395.

[166] A. G. Garcia, P. P. Lopes, J. F. Gomes, C. Pires, E. B. Ferreira, R. G. M. Lucena, L. H. S. Gasparotto, G. Tremiliosi-Filho, *New J. Chem.* **2014**, *38*, 2865–2873.

[167] N. Benipal, J. Qi, R. F. McSweeney, C. Liang, W. Li, *J. Power Sources* **2018**, *375*, 345–350.

[168] H. Xu, J. Wang, B. Yan, K. Zhang, S. Li, C. Wang, Y. Shiraishi, Y. Du, P. Yang, *Nanoscale* **2017**, *9*, 12996–13003.

[169] C. Jin, Z. Zhang, Z. Chen, Q. Chen, *Int. J. Electrochem. Sci.* **2013**, *8*, 4215–4224.

[170] N. Erini, R. Loukrakpam, V. Petkov, E. A. Baranova, R. Yang, D. Teschner, Y. Huang, S. R. Brankovic, P. Strasser, *ACS Catal.* **2014**, *4*, 1859–1867.

[171] R. F. De Souza, L. S. Parreira, D. C. Rascio, J. C. Silva, E. Teixeira-Neto, M. L. Calegaro, E. V. Spinace, A. O. Neto, M. C. Santos, *J. Power Sources* **2010**, *195*, 1589–1593.

[172] M. M. S. Pupo, F. E. López-Suárez, A. Bueno-López, C. T. Meneses, K. I. B. Eguiluz, G. R. Salazar-Banda, *J. Appl. Electrochem.* **2015**, *45*, 139–150.

[173] M. V. Pagliaro, M. Bellini, M. Bevilacqua, J. Filippi, M. G. Folliero, A. Marchionni, H. A. Miller, W. Oberhauser, S. Caporali, M. Innocenti, F. Vizza, *RSC Adv.* **2017**, *7*, 13971–13978.

[174] R. G. Da Silva, S. Aquino Neto, K. B. Kokoh, A. R. De Andrade, *J. Power Sources* **2017**, *351*, 174–182.

[175] S. Dash, N. Munichandraiah, *Electrochim. Acta* **2015**, *180*, 339–352.

[176] F. Colmati, E. Antolini, E. R. Gonzalez, *J. Power Sources* **2006**, *157*, 98–103.

[177] C. Wang, Y. Rong, T. Y. Hsu, *Mater. Sci.-Pol.* **2006**, *24*, 351–356.

[178] D. Lee, Y. Kim, Y. Kwon, J. Lee, T. W. Kim, Y. Noh, W. B. Kim, M. H. Seo, K. Kim, H. J. Kim, *Appl. Catal., B* **2019**, *245*, 555–568.

[179] B. Ran, S. Liu, J. Zhao, T. Tan, B. Liang, W. Wang, *J. Mater. Sci.* **2019**, *54*, 4579–4588.

[180] Y. Fan, B. R. Goldsmith, P. G. Collins, *Nat. Mater.* **2005**, *4*, 906–911.

[181] D. Hiltrop, S. Cychy, K. Elumeeva, W. Schuhmann, M. Muhler, *Beilstein J. Org. Chem.* **2018**, *14*, 1428–1435.